



**NAVAL
POSTGRADUATE
SCHOOL**

MONTEREY, CALIFORNIA

THESIS

**DESIGN OF A LIFT FAN ENGINE FOR A HEAVY LIFT
AIRCRAFT**

by

James E. Goebel

December 2003

Thesis Advisor:
Second Reader:

Raymond Shreeve
E. R. Wood

Approved for public release; distribution is unlimited

THIS PAGE INTENTIONALLY LEFT BLANK

REPORT DOCUMENTATION PAGE			Form Approved OMB No. 0704-0188	
Public reporting burden for this collection of information is estimated to average 1 hour per response, including the time for reviewing instruction, searching existing data sources, gathering and maintaining the data needed, and completing and reviewing the collection of information. Send comments regarding this burden estimate or any other aspect of this collection of information, including suggestions for reducing this burden, to Washington headquarters Services, Directorate for Information Operations and Reports, 1215 Jefferson Davis Highway, Suite 1204, Arlington, VA 22202-4302, and to the Office of Management and Budget, Paperwork Reduction Project (0704-0188) Washington DC 20503.				
1. AGENCY USE ONLY (Leave blank)		2. REPORT DATE December 03	3. REPORT TYPE AND DATES COVERED Master's Thesis	
4. TITLE AND SUBTITLE: Design of a Lift Fan Engine for a Heavy Lift Aircraft			5. FUNDING NUMBERS	
6. AUTHOR(S) James E Goebel				
7. PERFORMING ORGANIZATION NAME(S) AND ADDRESS(ES) Naval Postgraduate School Monterey, CA 93943-5000			8. PERFORMING ORGANIZATION REPORT NUMBER	
9. SPONSORING /MONITORING AGENCY NAME(S) AND ADDRESS(ES) N/A			10. SPONSORING/MONITORING AGENCY REPORT NUMBER	
11. SUPPLEMENTARY NOTES The views expressed in this thesis are those of the author and do not reflect the official policy or position of the Department of Defense or the U.S. Government.				
12a. DISTRIBUTION / AVAILABILITY STATEMENT Approved for public release; distribution is unlimited			12b. DISTRIBUTION CODE	
13. ABSTRACT (maximum 200 words) Recent conflicts have highlighted the difficulties in using aircraft to supply troops in modern warfare. Lift fan technology is seen as one way in which to improve future supply aircraft to meet the needs of the military. A previous study designed a heavy lift aircraft with lift fan engines that used future engine technology. This present study modified the design by using current engine technology for the lift fan engines. The modification is important because a design that uses current technology is more likely to be brought into service in the near future. This thesis documents the process required to use current technology in a lift fan engine for a heavy lift aircraft. The process uses current software and focuses on the design of the following components: the powerplant, the transmission shafts and the lift fan. The result is a propulsion system which allows a 185,000 lb aircraft to takeoff vertically as well as cruise at speeds greater than Mach=0.6.				
14. SUBJECT TERMS Heavy Lift Aircraft, Lift Fan Engine, Lift Fan			15. NUMBER OF PAGES 75	
			16. PRICE CODE	
17. SECURITY CLASSIFICATION OF REPORT Unclassified	18. SECURITY CLASSIFICATION OF THIS PAGE Unclassified	19. SECURITY CLASSIFICATION OF ABSTRACT Unclassified	20. LIMITATION OF ABSTRACT UL	

THIS PAGE INTENTIONALLY LEFT BLANK

Approved for public release; distribution is unlimited

DESIGN OF A LIFT FAN ENGINE FOR A HEAVY LIFT AIRCRAFT

James E Goebel
Commander, United States Navy
B.S., University of Notre Dame, 1988

Submitted in partial fulfillment of the
requirements for the degree of

MASTER SCIENCE IN AERONAUTICAL ENGINEERING

from the

**NAVAL POSTGRADUATE SCHOOL
December 2003**

Author: James E. Goebel

Approved by: Dr. Raymond Shreeve
Thesis Advisor

Dr. E. R. Wood
Second Reader/Co-Advisor

Anthony J. Healey
Chairman, Department of Mechanical and Astronautical
Engineering

THIS PAGE INTENTIONALLY LEFT BLANK

ABSTRACT

Recent conflicts have highlighted the difficulties in using aircraft to supply troops in modern warfare. Lift fan technology is seen as one way in which to improve future supply aircraft to meet the needs of the military. A previous study designed a heavy lift aircraft with lift fan engines that used future engine technology. This present study modified the design by using current engine technology for the lift fan engines. The modification is important because a design that uses current technology is more likely to be brought into service in the near future.

This thesis documents the process required to use current technology in a lift fan engine for a heavy lift aircraft. The process uses current software and focuses on the design of the following components: the powerplant, the transmission shafts and the lift fan. The result is a propulsion system which allows a 185,000 lb aircraft to takeoff vertically as well as cruise at speeds greater than Mach=0.6.

THIS PAGE INTENTIONALLY LEFT BLANK

TABLE OF CONTENTS

I.	INTRODUCTION.....	1
	A. BACKGROUND	1
	B. COMPONENTS.....	1
	C. BASELINE AIRCRAFT	1
	D. PERFORMANCE ESTIMATES.....	2
	1. Background	2
	2. Results	2
	E. ENGINE PERFORMANCE CALCULATIONS.....	3
	F. INSTALLED ENGINE PERFORMANCE	4
II.	POWERPLANT	5
	A. DESIGN CONSIDERATIONS.....	5
	B. BASELINE ENGINE.....	6
	C. CHANGES TO THE BASELINE ENGINE	6
	D. DERIVATIVE ENGINE	7
	1. Referencing Engine Performance to New Design Point	7
	2. Turbine and Nozzle Changes	8
	3. Engine Changes with Changes in LP Mechanical Efficiency	9
	4. Selection of the Derivative Engine Design Point	12
	E. ENGINE PERFORMANCE IN CRUISE.....	13
	1. Design Considerations	13
	2. Cruise Performance.....	14
	F. BLEED AIR.....	16
III.	TRANSMISSION SHAFTS	19
	A. DESIGN CONSIDERATIONS.....	19
	B. FAN AND SHAFT ROTATIONAL SPEED	19
	C. TRANSMISSION SHAFT THICKNESS.....	20
	1. Governing Equations	20
	2. Shaft Design.....	21
	C. TRANSMISSION SHAFT LENGTH	22
	1. Critical Speed	22
	2. Governing Equations	22
	3. Actual Design.....	23
IV.	LIFT FAN	25
	A. DESIGN CONSIDERATIONS.....	25
	B. AEROTHERMODYNAMIC ANALYSIS.....	25
	C. LIFT FAN PRELIMINARY DESIGN.....	28
	1. Design Tool	28
	2. Determination of Initial Lift Fan Parameters.....	29
	a. Fan Blade Tip Speed (U_t)	29
	b. Inlet Relative Flow Angle (β_i).....	29

3.	Design of Lift Fan.....	30
a.	<i>Design Iteration</i>	30
b.	<i>Lift Fan Gearing</i>	30
c.	<i>Fan Designs</i>	31
V.	FINAL AIRCRAFT DESIGN.....	35
A.	ADDITION OF THRUST	35
1.	Requirement	35
2.	Solution	35
B.	DESIGN OF TRANSMISSION SHAFT	36
C.	FINAL AIRCRAFT DESIGN.....	37
VI.	CONCLUSIONS AND RECOMMENDATIONS.....	39
A.	CONCLUSIONS	39
B.	RECOMMENDATIONS.....	39
	LIST OF REFERENCES.....	41
	APPENDIX A.....	43
	APPENDIX B	47
	COMPONENT MAPS FOR 0 FEET AND M=0.0 (CRUISE)	47
	COMPONENT MAPS FOR 5000 FEET AND M=0.55 (CRUISE)	48
	COMPONENT MAPS FOR 20000 FEET AND M=0.6 (CRUISE)	49
	APPENDIX C	51
	INITIAL DISTRIBUTION LIST	59

LIST OF FIGURES

Figure 1.	Two Spool Mixed Flow Turbofan Engine Configuration.....	4
Figure 2.	Variation of Engine Thrust with A8	11
Figure 3.	Variation of Total LP SHP with A8.....	11
Figure 4.	GASTURB Limiters Selection Screen.....	13
Figure 5.	GASTURB Modifiers Selection Screen	14
Figure 6.	Engine Fan Map.....	15
Figure 7.	Engine LP Turbine Map.....	16
Figure 8.	Plot of Shaft Length Versus Natural Frequency	24
Figure 9.	Mass Flow vs Thrust.....	27
Figure 10.	Mass Flow vs Lift Fan Diameter	28
Figure 11.	Basic Blade Theory.....	29
Figure 12.	Lift Fan Engine Installation Dimensions	36
Figure 13.	Top View of Heavy Lift Aircraft.....	37
Figure 14.	Perspective View of Heavy Lift Aircraft.....	38

THIS PAGE INTENTIONALLY LEFT BLANK

LIST OF TABLES

Table 1.	Aircraft Characteristics	2
Table 2.	Aircraft Thrust and Fuel Requirements (Aircraft Weight: 180000 lbs)	3
Table 3.	Estimated Baseline Engine Parameters.....	6
Table 4.	Estimated Lift Engine Parameters	8
Table 5.	Variation of Engine Parameters with LP Mechanical Efficiency.....	10
Table 6.	Estimated Lift Engine Parameters	12
Table 7.	Cruise Performance for One Engine	15
Table 8.	Estimated Derivative Engine Parameters.....	17
Table 9.	Properties of Titanium Alloy (Ti-6Al-4V).....	21
Table 10.	Values Used for Calculation of Maximum Shear Stress	21
Table 11.	Values for a_n for Clamped-Clamped Beam.....	23
Table 12.	Initial Lift Fan Parameters	27
Table 13.	Lift Fan Design Constraints	30
Table 14.	Diameter vs Rotational Speed (Fan Blade Tip Speed=1632ft/s)	31
Table 15.	Potential Lift Fan Designs	32
Table 16.	Detailed Fan Design Parameters.....	33
Table 17.	Summary of Thrust Calculations	35
Table 18.	F-35C Engine Performance.....	35
Table 19.	Summary of Thrust Calculations	36

THIS PAGE INTENTIONALLY LEFT BLANK

ACKNOWLEDGMENTS

I would like to thank the following individuals for their guidance with this thesis:

Dr. Raymond Shreeve, Professor, Naval Postgraduate School

Dr. E. R. Wood, Professor, Naval Postgraduate School

Dr. Paul Bevilaqua, Manager of the Advanced Developmental Programs Division,
Lockheed Martin, Palmdale, CA

THIS PAGE INTENTIONALLY LEFT BLANK

I. INTRODUCTION

A. BACKGROUND

Recent conflicts have highlighted the difficulties of supplying troops in modern warfare. A problem with staging supplies in foreign countries has led the military to examine supplying troops directly from ships. A recent study at the Naval Postgraduate school outlined the requirements that a future cargo aircraft might face in this scenario: large enough to carry 37,500 pounds of cargo including vehicles; be able to cruise at relatively high speeds on missions up to 600 nautical miles; and be flexible enough to land and takeoff vertically (Erhardt, W., 2002). One proposal for this mission involved an aircraft that used lift fan engines (Wood, E. R., 2003). The present project attempted to improve on the aircraft outlined in the proposal by incorporating lift fan engines that require only modest changes to the engine designs. The approach taken is outlined in the following paragraphs.

B. COMPONENTS

The present project addressed the following components of the lift fan engine: the powerplant, the transmission shafts, and the lift fan. The thrust vectoring nozzle on the powerplant and the mechanical gearing that connected the transmission shaft to the lift fan were not addressed. However, after an examination of current technology the following assumptions were made about the unexamined components. First, a swiveling nozzle would direct the thrust of the powerplant vertically without loss when required for hover. Second, the rotational speed of the lift fan should be held to within 25% of the rotational speed of the low pressure (LP) engine spool in order to limit the size of the mechanical coupling.

C. BASELINE AIRCRAFT

The baseline aircraft was designed to have the characteristics shown in Table 1.

Table 1. Aircraft Characteristics

Aircraft Parameter	Value
Length (ft)	114
Width (ft)	13.2
Wing Span (ft)	96.6
Wing Chord at Root (ft)	25.6
Aircraft Weight with Two Lift Fan Engines (lbs)	82500
Maximum Cargo Weight (lbs)	37500
Maximum Aircraft Weight – With Two Engines, Without Fuel (lbs)	120000

D. PERFORMANCE ESTIMATES

1. Background

The drag and fuel figures for the baseline aircraft were calculated through the use of the AEDsys software program (Mattingly and Pratt). The software program required initial estimates for the weight of the aircraft (including fuel) and the thrust of the aircraft at sea level. For the software calculations, the total aircraft weight (including fuel) was estimated to be 180000 lbs. This number was determined by adding the maximum aircraft weight of 120000 lbs with an estimated aircraft fuel weight of 60000 lbs. In addition, the thrust was estimated to be 60000 lb_f. The estimates for aircraft weight and thrust were then used to calculate the drag and fuel used by the aircraft over the following flight profile: Vertical takeoff, conventional climb to 20000 feet, cruise leg at 20000 feet and M=0.6, and then, loiter for 15 minutes before landing vertically. The total distance covered during the climb and cruise was 300 nautical miles.

2. Results

The data for the flight profile are shown in Table 2. The data showed that 28000 lbs of fuel were required to complete one 300 nautical mile leg. The mission fuel

requirement (600 nautical miles total) was found on the assumption that the mission would involve two identical 300 nautical mile legs with a landing after each leg. Thus, the total mission fuel used was estimated to be 56,000 lbs. It was noted that the aircraft had a difficult time accelerating as shown by the large amount of fuel used in the climb. The fuel numbers indicated that although the aircraft functioned with a thrust of 60,000 lbs, a greater amount of thrust was desired.

Table 2. Aircraft Thrust and Fuel Requirements (Aircraft Weight: 180000 lbs)

Flight Profile	Drag (lbs)	Fuel (lbs)
Start and Hover for 2.5 min	175000	3000
Climb to 20000 feet (1)	~22500	11000
Cruise at 20000 feet / M=0.6 (1)	19500	7500
Loiter for 15 min at 5000 feet	15000	3500
Hover for 2.5 min and Land	175000	3000
Total Fuel for One 300 Nautical Mile Leg		28000
Note (1): The total distance covered during the climb and cruise is 300 nautical miles		

E. ENGINE PERFORMANCE CALCULATIONS

The program used to calculate the engine performance was GASTURB Version 9 (Copyright © 2001, Joachim Kuzke). The calculations were made using the Two Spool Mixed Flow Turbofan engine configuration in GASTURB. Figure 1 is a generic diagram of a Two Spool Mixed Flow Turbofan engine configuration and it gives the notation for stations within the engine.

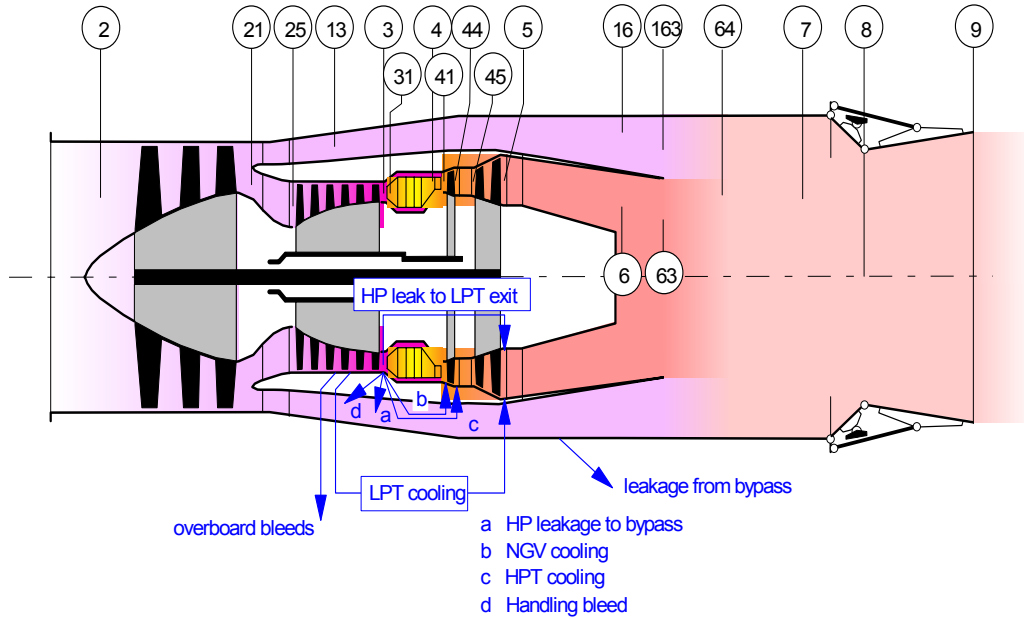


Figure 1. Two Spool Mixed Flow Turbofan Engine Configuration

F. INSTALLED ENGINE PERFORMANCE

The software programs used in the present project calculated the uninstalled thrust from the lift fan and the engine. The programs did not take into account the loss of thrust once the engine and lift fans were installed into the aircraft. Since there was no established way to calculate the installed thrust, it was assumed that there was a 10% difference between the uninstalled thrust and the installed thrust. For all calculations of thrust, the uninstalled thrust was reduced by 10% to provide a value for the installed thrust of the aircraft.

II. POWERPLANT

A. DESIGN CONSIDERATIONS

There were two options when determining the powerplant for a lift fan engine: alter an existing engine or design a new one. The present study focused on altering an existing engine because it was viewed as the most realistic approach. Although the engine would not provide the optimum design, it would result in a system more likely to reach service in the near future.

The engine for the F-35C is currently the only lift fan that is approaching operational status. The engine is a low bypass turbofan engine that has provisions for driving the lift fan from the Low Pressure (LP) engine spool. Equation 1 is the expression of the balance of power between the turbine and the core compressor, bypass fan and lift fan.

$$\left(\frac{1+f}{1+\alpha}\right)C_{p_t}(T_{t_3}-T_{t_2}) = \frac{C_{p_c}(T_{t_3}-T_{t_2})}{(1+\alpha)} + \left(\frac{\alpha}{1+\alpha}\right)C_{p_c}(T_{t_{13}}-T_{t_2}) + \left(\frac{P_{LF}}{m_o}\right) \quad (1)$$

where f =fuel to air ratio, α =bypass ratio, C_p =ratio of specific heats in the turbine (t) and compressor (c), T_t =stagnation temperatures at the stations depicted in Figure 1, P_{LF} =Power to the lift fan, and m_o =engine air flow rate. If the turbine is designed for the engine without a lift fan, it must operate far from its design point when the lift fan is engaged. If it is designed for operation with the lift fan engaged, it will be far off design when the lift fan is disengaged.

In conducting the present study, the low bypass ratio (α) of the current engine was accepted, but a larger fraction of the turbine power was required for the lift fan. This required proposing a modification of the turbine, and changing the nominal design point to be in hover.

B. BASELINE ENGINE

The baseline engine used to begin the study was one created to approximate the engine in the F-35C. The engine specified had a low bypass ratio and high performance characteristics. The F-35C engine specifications were not available, but representative specifications for the technology level of the engine were estimated as shown in Table 3. The complete list of engine parameters entered into the GASTURB program is given in Appendix A.

Table 3. Estimated Baseline Engine Parameters

Engine Parameter	Value
Design Point	30000 feet and M=1.47
Bypass Ratio	0.30
Inlet Corrected Mass Flow (lbm/sec)	370
Inner Fan Pressure Ratio	5
Outer Fan Pressure Ratio	5
High Pressure Compressor Pressure Ratio	6.4
Maximum Burner Temperature (°R)	3760
Low Pressure Turbine Pressure Ratio	2.017
A_8 (in ²)	444.39
Thrust at Design Point (lb _f)	23599
Length	20 feet
Hub to tip ratio	0.40

C. CHANGES TO THE BASELINE ENGINE

The baseline engine had a pressure ratio of 1.8 across the LP turbine. Since the pressure ratio needed to be increased in order to increase the work output of the turbine, a redesign of the turbine was proposed. Other than the modification of the turbine, all the

other turbo-machinery components of the baseline engine were incorporated into the new engine.

Also, the baseline engine was intended for a high performance aircraft with a nominal design point at 30000 feet and $M=1.47$. Because the main focus of the heavy transport aircraft was a vertical takeoff, the derivative engine was designed to achieve maximum performance at 0 feet and $M=0.0$. In addition, the engine was optimized for hover operations where work was being drawn off the turbine to power the lift fan. Although this meant that the engine would run inefficiently in cruise, the tradeoff was needed to maximize the hover performance.

D. DERIVATIVE ENGINE

1. Referencing Engine Performance to New Design Point

The first step in the redesign process was to re-reference the performance of the engine from its original design point to its new design point using the software program GASTURB. The baseline engine, with a design point at 30,000 ft and $M=1.47$, was run off design at 0 feet and $M=0.0$. During the run the corrected high pressure spool speed and the corrected low pressure spool speed were limited to 100%. The off-design performance parameters at 0 feet and $M=0.0$ are listed in the first column in Table 4.

Table 4. Estimated Lift Engine Parameters

Engine Parameter	Baseline Engine Off Design	Derivative Engine at Design Point
Flight Condition	0 Feet, M=0.0	0 Feet, M=0.0
Bypass Ratio	0.308	0.308
Inlet Corrected Mass Flow (lbm/sec)	369.635	369.635
Inner Fan Pressure Ratio	4.966	4.966
Outer Fan Pressure Ratio	4.966	4.966
High Pressure Compressor Pressure Ratio	6.4	6.4
Maximum Burner Temperature (°F)	3347	3760
Low Pressure Turbine Pressure Ratio	2.016	1.818
A_8 (in ²)	444.39	454
Thrust (lb _f)	33767	37402
LP Shaft Horse-power (SHP)	42533	42546

The basic parameters governing the inner fan, outer fan and high pressure compressor were taken from the off-design case and used in the new design point as shown in Table 4. These numbers ensured that the all of the components except the turbine operated in the same manner. This process left the turbine as the only turbo-machinery component to be redesigned.

2. Turbine and Nozzle Changes

The second step in the redesign was establishing a process that altered the engine to produce excess work out of the turbine to power the lift fan. The component of the engine most responsible for the control of the turbine work output was the area at station

8 (A_8) (see Figure 1). Increasing A_8 increased the pressure drop across the turbine and resulted in an increase in work produced by the turbine. As long as the increased work was drawn off to power the lift fan, all other components of the engine functioned as before. The process of altering A_8 and controlling the turbine work output was accomplished using the LP spool mechanical efficiency parameter in the GASTURB program. Although the LP spool mechanical efficiency parameter did not affect a physical engine component, reducing the parameter properly simulated the extraction of shaft power for a lift fan.

3. Engine Changes with Changes in LP Mechanical Efficiency

Table 5 shows how the parameters of the engine varied with a change in the LP spool mechanical efficiency (e). Figures 2 and 3 show the variation of engine thrust (FN), and total SHP with the size of A_8 . As A_8 was increased the Low Pressure Turbine Pressure Ratio increased. The increase in the pressure ratio resulted in an increase in the total SHP produced by the LP Spool. Since only 44440 SHP was required to drive the engine fan, the increased work was removed to provide power to the lift fan, as shown by the available SHP. The figures show that an increase in A_8 resulted in a small loss of engine thrust, but a significant increase in the SHP available for the lift fan.

Table 5. Variation of Engine Parameters with LP Mechanical Efficiency

LP Mechanical Efficiency (ϵ)	A_8 (in ²)	Thrust (lbf)	Low Pressure Turbine Pressure Ratio	Total LP SHP	LP SHP Available for Lift Fan
1.00	454	37402	1.818	42546	0
0.95	456	37191	1.880	44786	2239
0.90	459	36952	1.953	47274	4727
0.85	462	36677	2.038	50054	7508
0.80	467	36358	2.139	53183	10637
0.75	473	35981	2.261	56728	14182
0.70	482	35524	2.411	60780	18234
0.65	499	34929	2.600	65435	22910
0.60	536	34099	2.844	70910	28364
0.55	587	33022	3.169	77357	34811
0.50	658	31598	3.622	85092	42546

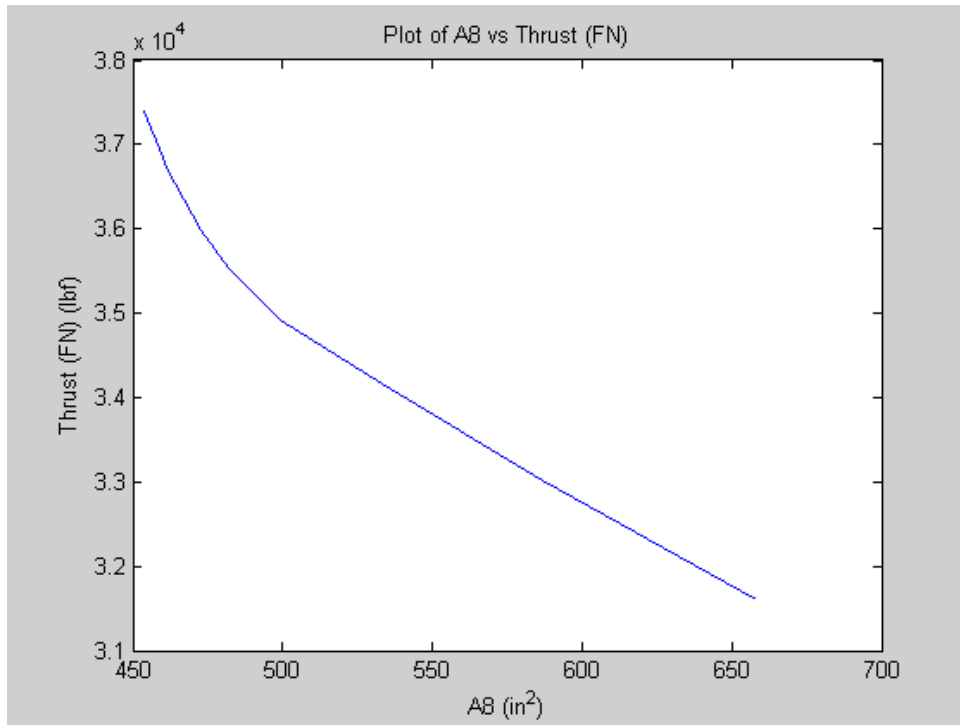


Figure 2. Variation of Engine Thrust with A8

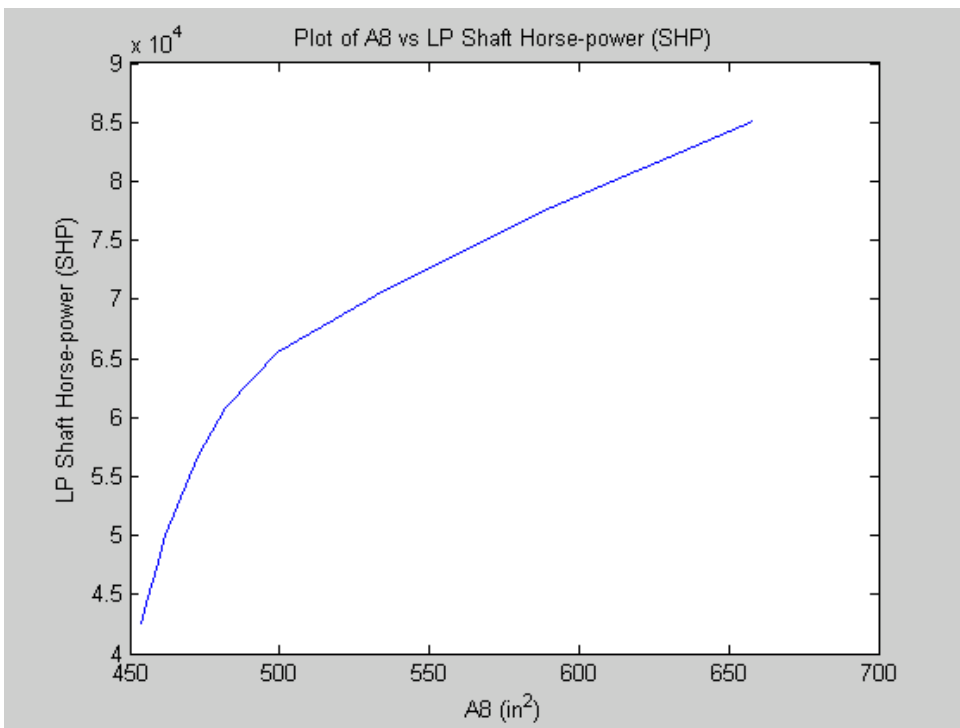


Figure 3. Variation of Total LP SHP with A8

4. Selection of the Derivative Engine Design Point

Because the designed called for the thrust produced in hover to be fairly well balanced between the lift fan and the engine, a mechanical efficiency of 0.6 was chosen for the design point of the engine. The final design parameters of the engine are those in Table 6.

Table 6. Estimated Lift Engine Parameters

Engine Parameter	
Design Point	0 feet and M=0.0
Bypass Ratio	0.308
Inlet Corrected Mass Flow (lbm/sec)	369.635
Inner Fan Pressure Ratio	4.966
Outer Fan Pressure Ratio	4.966
High Pressure Compressor Pressure Ratio	6.4
Maximum Burner Temperature (°F)	3760
Low Pressure Turbine Pressure Ratio	2.844
A_8 (in ²)	536
Thrust at Design Point (lb _f)	34099
LP Shaft Horse-power (SHP)	70910
LP Shaft Horse-power (SHP) Available for Lift Fan	28364
Length	20 feet
Hub to tip ratio	0.40

E. ENGINE PERFORMANCE IN CRUISE

1. Design Considerations

As stated earlier, the engine was optimized for the hover case in that it was designed for zero altitude, $M=0.0$ with a LP spool power take-off of 40% for the lift fan. For all other operating points, the engine was operated off-design. In cruise, because the lift fan no longer drew power from the engine, the LP spool mechanical efficiency was required to be set at 99%. The increased mechanical efficiency altered the engine performance since the work that the turbine was designed to produce was no longer required. The additional work was absorbed by the bypass fan. This required that the Low Pressure Spool Speed in GASTURB be limited to ensure that the engine fan and the LP Turbine operated at acceptable points on the associated component maps, and always below the design spool speed. In addition, the nozzle area was required to be adjusted at each off-design point to ensure that the work balance between the engine fan and the LP turbine was such that engine fan provided a high pressure ratio at a high efficiency. Figure 4 and 5 show the input screens in GASTURB that allowed the variation of the Low Pressure Spool Speed and the nozzle to be controlled. The final choices of Low Pressure Spool Speed and nozzle area were based on selecting the combination that provided the greatest thrust from the engine.

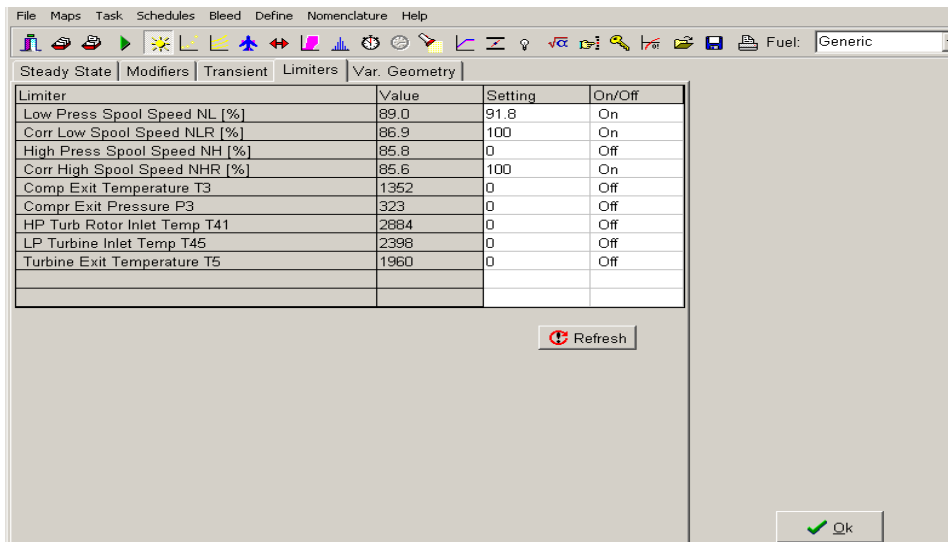


Figure 4. GASTURB Limiters Selection Screen

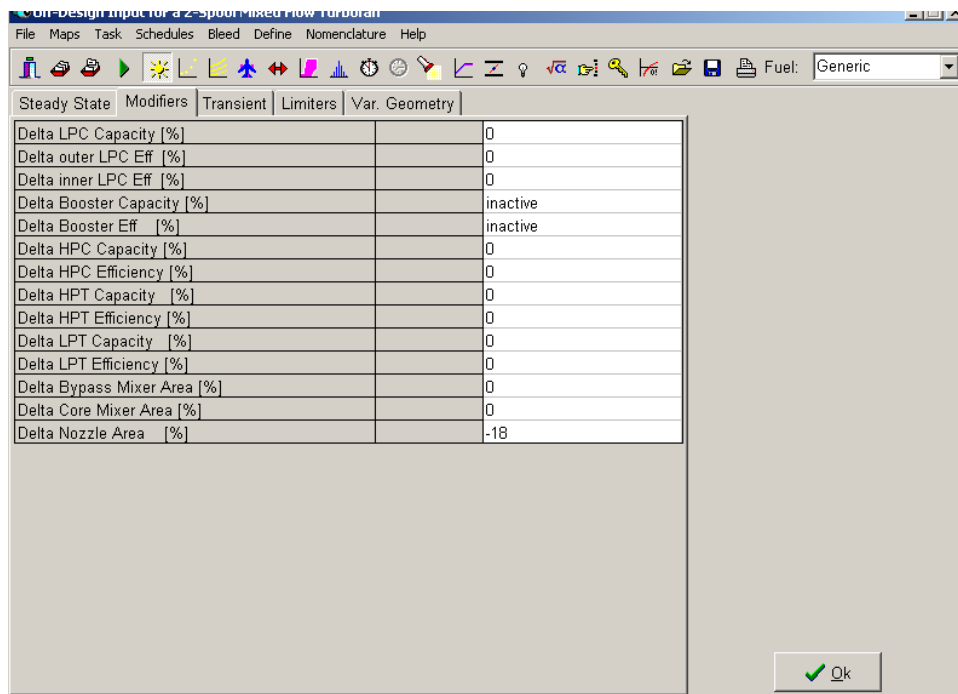


Figure 5. GASTURB Modifiers Selection Screen

2. Cruise Performance

Table 7 shows the performance of one derivative engine at three forward thrust operating conditions. Figure 6 and 7 show component maps for the engine fan and LP turbine respectively with the operating condition at 20000 ft and $M=0.6$. The remainder of the engine component maps and operating conditions for the points in Table 7 are given in Appendix B. The data indicated that the derivative engine had enough thrust such that only two engines were required to operate the aircraft up to approximately 20000 feet. The small difference between the thrust available and the thrust required, though, indicated that aircraft would have a difficult time accelerating. If the aircraft was required to have greater performance or be operated above 20000 feet then the aircraft would require additional thrust. It can be seen in Figure 6 that the LP compressor operating point was relatively near the stall line of the compressor. This was considered acceptable because the mission of the aircraft would not require the engine to operate under flight conditions where the throttle would be changed rapidly.

Table 7. Cruise Performance for One Engine

Cruise Condition	Change in Nozzle Area (%)	Maximum LP Spool Speed (rpm)	Uninstalled Thrust Available (lbf)	Installed Thrust Available (lbf)	Total Installed Thrust Available (lbf)	Thrust Required for Aircraft (lbf)
0 ft M=0.0	-2	86.9	20540	18490	36980	N/A
5000 ft M=0.55	-14	92.7	17972	16172	32344	25400
20000 ft M=0.6	-18	91.8	12300	11070	22140	19500

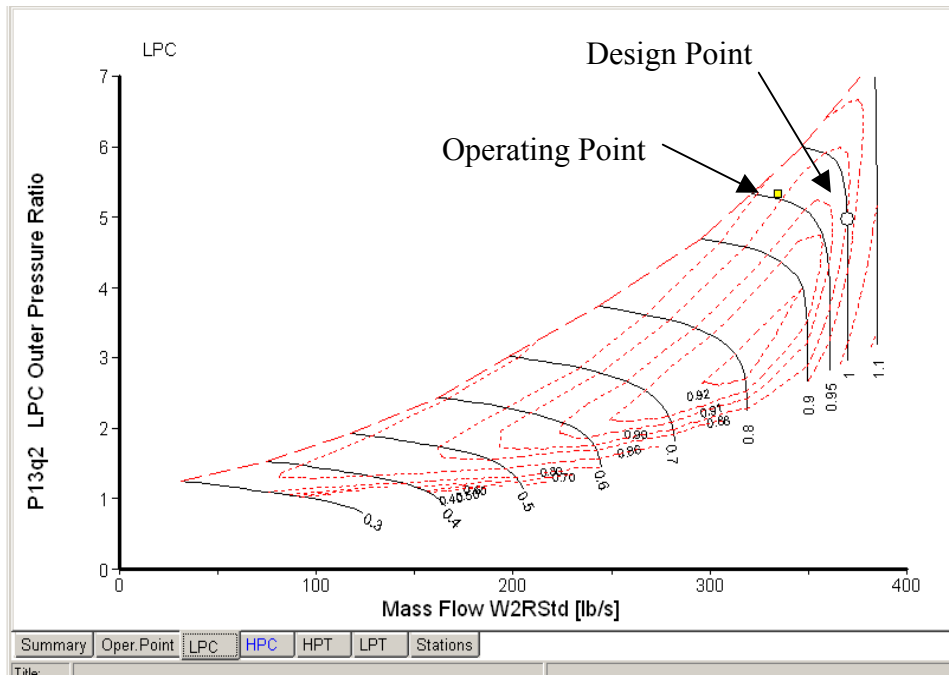


Figure 6. Engine Fan Map

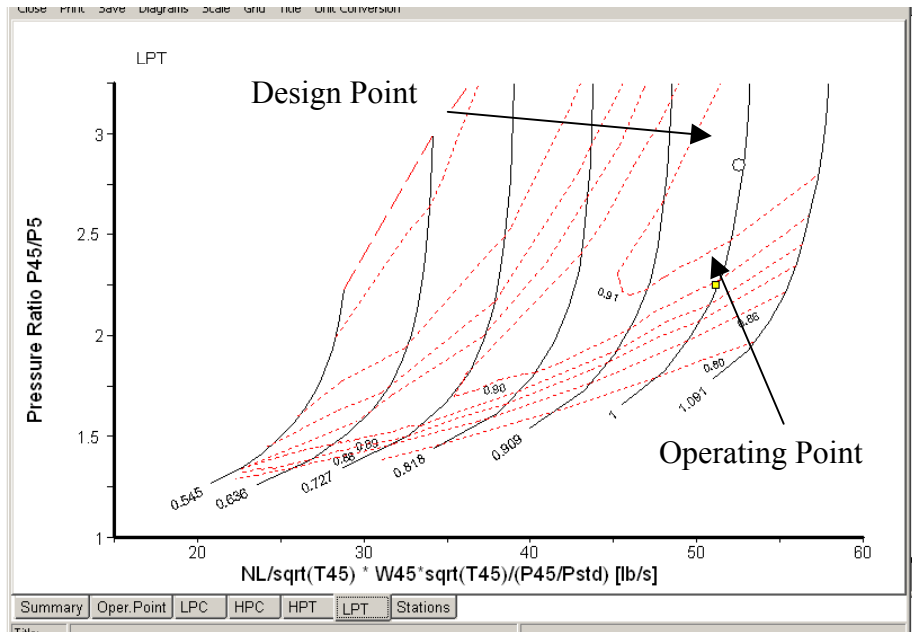


Figure 7. Engine LP Turbine Map

F. BLEED AIR

The baseling engine had an A_8 of 444 in², as shown in Table 3. The derivative lift fan engine had an A_8 of 536 in² as shown in Table 6. The difference of 92 in² represented a significant increase over the original design. Although it was not determined to be necessary for the present design, there was an alternate way to achieve the desired work out of the engine without using as large an increase in A_8 . The method involved taking the bypass air from the fan and bleeding it overboard. In GASTURB, the parameter was called the Relative Fan Overboard Bleed (W_{Bld}/W_{13}). Table 8 showed an alternative derivative engine design that utilized bypass air being bled overboard. The bleed air method worked because it reduced the mass flow at A_8 for the same turbine pressure ratio and flow rate. Thus, A_8 was not required to be as large. The information in Table 8 showed that if 99% of the bypass air was bled overboard through an auxiliary nozzle, the required A_8 was only 457 inches with the same LP shaft-horsepower generated. In addition, the air bled overboard could be used as additional thrust, or for directional control. Assuming that the auxiliary nozzle was convergent, Table 8 showed that the overboard bypass air generated 2717 lb_f of thrust.

Table 8. Estimated Derivative Engine Parameters

Engine Parameter	Design Point – Single Thrust Nozzle	Design Point with Fan Bleed Air Nozzle
Design Point	0 feet and M=0.0	0 Feet, M=0.0
Bypass Ratio	0.308	0.308
Inlet Corrected Mass Flow (lbm/sec)	369.635	369.635
Inner Fan Pressure Ratio	4.966	4.966
Outer Fan Pressure Ratio	4.966	4.966
High Pressure Compressor Pressure Ratio	6.4	6.4
Maximum Burner Temperature (°F)	3760	3760
Low Pressure Turbine Pressure Ratio	2.844	1.818
Relative Fan Overboard Bleed (W13)	0%	99%
A_8 (in ²)	536	457
Thrust at Design Point (lb _f)	34099	29161
LP Shaft Horse-power (SHP)	70910	70910
Mass Flow from Overboard Bleed (lbm/s)	0	78.3
Thrust from Overboard Bleed (lb _f)	0	2717
Total Uninstalled Thrust from Engine (lb _f)	34099	31878
Total Installed Thrust from Engine (lb _f)	30700	28700

THIS PAGE INTENTIONALLY LEFT BLANK

III. TRANSMISSION SHAFTS

A. DESIGN CONSIDERATIONS

A transmission shaft connected the powerplant to the lift fan. The design of the transmission shaft was important because lift fan engines in general required transmission of relatively large amounts of power from the powerplant. In addition, the transmission shaft's length, thickness and weight had an impact on the overall design of the aircraft. Thus, the transmission shaft design was an integral part when designing a lift fan engine.

B. FAN AND SHAFT ROTATIONAL SPEED

Because the transmission shaft was an extension of the Low Pressure (LP) engine spool, the design of the shaft was dictated by the rotational speed of the LP engine spool. The determining factor in the LP engine spool speed was the maximum centrifugal tensile stress of the fan blade. The stress was based primarily on the material of the blade, the flowpath throughflow area and the blade's centrifugal acceleration (Mattingly, Heiser and Pratt, 2002). The relationship between these factors is shown in equation 2

$$AN^2 = \frac{3600\sigma_c}{\pi(1 + \frac{A_t}{A_h})\rho} \quad (2)$$

where A is the flowpath throughflow area in in², N is the rotational speed in rpm, σ_c is the maximum allowable tensile stress, ρ is the density of the material and A_t/A_h is the taper ratio of the blade (assumed to be 0.8). Based on current titanium blade technology the value for σ_c was estimated to be 70000 ksi and the value for ρ was taken to be 9.08 slug/ft³. Using these values in equation 2 resulted in a value of 1.00×10^{11} in²-rpm² for AN^2 . The throughflow area was calculated using

$$A = \pi R_t^2 (1 - (\frac{R_h}{R_t})^2) \quad (3)$$

where R_t was the radius of the fan blade at the tip and R_h/R_t was the ratio of the hub radius to tip radius. Examining current technology, representative values for R_t and R_h/R_t

were 39 inches and 0.4 respectively. Inserting these values into equations 2 and 3 resulted in a calculation of 10,000 rpm for the rotation speed of the engine.

C. TRANSMISSION SHAFT THICKNESS

1. Governing Equations

The rotational speed of the LP spool and the shaft horsepower transmitted to the lift fan were used to determine the diameter of the shaft and the thickness of the shaft wall. The rotational speed (N) and the shaft horsepower (SHP) were related to the torque (T) generated by the shaft by

$$T = \frac{SHP * 63025}{N} \quad (4)$$

The torque was then related to the shear stress (τ) generated on the shaft with a thin walled closed circular section using (Allen and Haisler, 1985)

$$\tau = \frac{2Tr_o}{\pi(r_o^4 - r_i^4)} \quad (5)$$

where r_o is the outer radius of the circular section and r_i is the inner radius of the circular cross section. Combining the two equations, the shear stress in the shaft was related to the dimensions of the shaft, the shaft-horsepower transmitted by the shaft and the rotational speed of the shaft, as

$$\tau = \frac{126050 * SHP * r_o}{N\pi(r_o^4 - r_i^4)} \quad (6)$$

Since the shaft-horsepower and the rotational speed were determined in the design of the powerplant, the size of the shaft (and thickness) were required to be large enough to ensure that the maximum allowable shear stress in the shaft was not exceeded.

2. Shaft Design

Since the transmission shaft was an extension of the LP engine spool, the shaft was modeled with similar dimensions and materials as the LP engine spool. Based on current technology for an engine with a 39 inch fan diameter and a fan blade hub-to-tip ratio of 0.4, the derivative engine was estimated to have a LP drive shaft diameter of 5 inches and a shaft wall thickness of 0.25 inches. A titanium alloy (Ti-6Al-4V) was assumed. The properties of the alloy are shown in Table 9.

Table 9. Properties of Titanium Alloy (Ti-6Al-4V)

Material	Modulus of Elasticity (E) (Mpsi)	Unit Weight (w) (lb/in ³)	Yield Shear Stress (τ) (ksi)
Titanium Alloy (Ti-6Al-4V)	17.4	.16	87

Using equation 6 with the values shown in Table 10, the maximum shear stress for the transmission shaft was calculated to be 21 ksi.

Table 10. Values Used for Calculation of Maximum Shear Stress

Outer Radius (r_o) (in)	Inner Radius (r_i) (in)	SHP	N (rpm)	Maximum Shear Stress (τ) (ksi)
2.5	2.25	28300	10000	21

The maximum shear stress of 21 ksi was well below the maximum yield shear stress. The calculations indicated that the size of the transmission shaft was appropriate for the power transmitted to the lift fan. It was noted, however, that the baseline engine LP drive shaft was designed to transmit 42,500 shp. The additional 28,300 shp supplied to the

lifting fan was a 40% increase from the original design. These numbers indicated that the thickness of the derivative engine drive shaft would have to be increased slightly to compensate for the increased power.

C. TRANSMISSION SHAFT LENGTH

1. Critical Speed

The length of the transmission shaft was defined as the length from the fan on the powerplant to the gearbox located on the lift fan. The primary consideration in designing the length of the transmission shaft was the critical speed of the shaft. Because the shaft was rotating, centrifugal forces acted on the shaft. A perturbation of the centrifugal force could be resolved into horizontal and vertical components that would trigger vertical and horizontal vibrations of the shaft. The vibrations become violent when the angular speed of the shaft coincides with the natural frequency of the non-rotating shaft (Den Hartog, J.P., 1985). This angular speed is referred to as the critical speed.

2. Governing Equations

The natural frequency of the rotating shaft (ω_n) depends on the material of the shaft and the length of the shaft (l) as

$$\omega_n = a_n \sqrt{\frac{EI}{\mu l^4}} \quad (7)$$

where a_n is a numerical constant which varies with the boundary conditions of the shaft, E is the Modulus of Elasticity, I is the Moment of Inertia, and μ is the mass per unit length. I and μ are given by

$$I = \frac{\pi}{4} (r_o^4 - r_i^4) \quad (8)$$

and

$$\mu = \frac{w * \pi (r_o^2 - r_i^2)}{gl} \quad (9)$$

where w is specific weight of the material and g is the gravitational constant (386.09 in/s²). Combining equations 7, 8 and 9 and inserting the value for g gives

$$\omega_n = a_n \sqrt{\frac{193.044 * E (r_o^4 - r_i^4)}{w (r_o^2 - r_i^2) l^3}} \quad (10)$$

Since the rotational speed of the shaft was known, equation 10 was used to determine the length of the shaft that resulted in a natural frequency that avoided the rotational speed of the shaft.

3. Actual Design

Since the shaft was constrained at the fan of the powerplant and the gearbox of the lift fan, the shaft was modeled initially as a single ‘clamped-clamped’ beam. Solving the Bernoulli-Euler equation for a beam clamped at both ends, the values for a_n are those shown in Table 11.

Table 11. Values for a_n for Clamped-Clamped Beam

Node	1	2	3	4
Value for a _n	22.373	61.670	120.912	199.855

Inserting the values for a_n along with the material properties of the alloy and plotting the natural frequency versus length resulted in the graph shown in Figure 8.

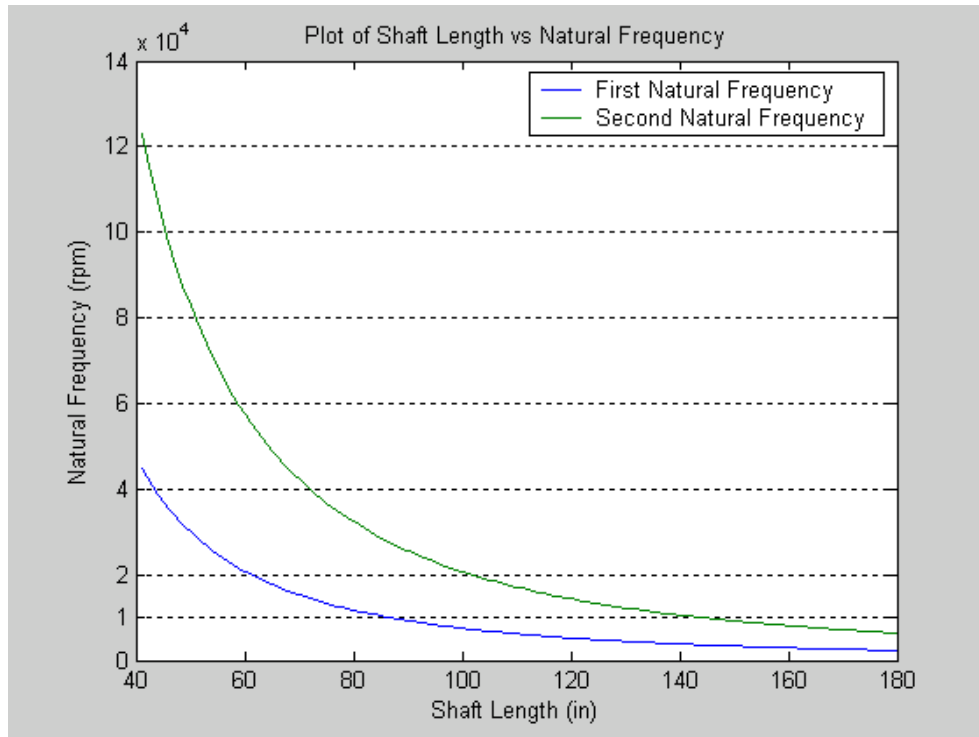


Figure 8. Plot of Shaft Length Versus Natural Frequency

The figure demonstrated that the rotational speed of 10000 rpm for the transmission shaft approached the natural frequency of a ‘clamped-clamped’ shaft at lengths of approximately 90 inches. In order for the shaft to operate effectively it would have to be designed to be shorter or longer than 90 inches. The behavior of the beam at the second natural frequency was not considered because 90 inches was felt to be the largest length for a possible shaft design. It should be noted that although there were many options for modeling the shaft such as two ‘clamped-free’ beams coupled together, these options were not considered due to the ability of the ‘clamped-clamped’ beam to meet the desired design goals.

IV. LIFT FAN

A. DESIGN CONSIDERATIONS

The lift fan was required to turn the shaft horsepower generated by the powerplant into useful vertical thrust for the aircraft. Because the fan was mounted horizontally, it gave rise to a number of questions. The primary one was whether the lift fan could produce the required thrust. The second question concerned the dimensions of the resulting fan with respect to the limited space on the aircraft. The lift fan not only was required to provide the needed thrust, but it was required to do so in a size that would be compatible with the aircraft.

B. AEROTHERMODYNAMIC ANALYSIS

The first step in the design was an aerothermodynamic analysis to determine the approximate parameters of the lift fan. The analysis used one-dimensional equations to describe the performance of a generic fan. In order to calculate lift fan thrust (T_f), the parameters required to be specified were: shaft horsepower supplied to the lift fan (SHP), diameter (D), hub-to-tip ratio (R_h/R_t), axial mach number (M_{a1}), inlet stagnation temperature (T_{t1}), inlet stagnation pressure (P_{t1}), inlet pressure loss (π_d), nozzle pressure loss (π_n), and fan polytropic efficiency (e_f). The sequence of equations included the expression for the fan face area,

$$A_1 = \frac{\pi D^2}{4} \left(1 - \frac{R_h}{R_t}\right)^2 \quad (11)$$

the flow rate through the fan,

$$\dot{m}_f = \frac{P_{t1} A_1 g_c}{\sqrt{\gamma R T_{t1} g_c}} \gamma M_{a1} \left(1 + \frac{\gamma - 1}{2} M_{a1}^2\right)^{\frac{-(\gamma + 1)}{2(\gamma - 1)}} \quad (12)$$

the power required by the fan,

$$SHP = \dot{m}_f C_p T_{t1} (\tau_f - 1) * \frac{778}{550} \quad (13)$$

the relationship between fan pressure and temperature ratio,

$$\tau_f = \pi_f^{\frac{\gamma-1}{\gamma e_f}} \quad (14)$$

and the expression for the specific thrust if the fan nozzle is correctly expanded to atmospheric pressure.

$$ST_f = \sqrt{\left(\frac{2\gamma}{\gamma-1}\right)\left(\frac{RT_{t1}}{g_c}\right) \frac{\pi_f^{\frac{(\gamma-1)(1-e_f)}{\gamma e_f}}}{(\pi_d \pi_n)^{\frac{\gamma-1}{\gamma}}} [(\pi_f \pi_d \pi_n)^{\frac{\gamma-1}{\gamma}} - 1]} \quad (15)$$

Then, the total thrust from the lift fan is given by

$$T_f = \dot{m} ST_f \quad (16)$$

Examining current technology and using the available values of SHP fixed the parameters shown in Table 12. That left the thrust to depend on the parameters of D and M_{a1} . It was assumed that there were two engines, with each lift fan required to have a thrust of 55000 lbf in order for the aircraft to hover. Figure 9 shows the variation of thrust with mass flow. Figure 10 shows the variation of mass flow with D and M_{a1} at an inlet pressure of 14.7 psi. By examining the two figures in order, it was seen that 55000 lbf required a mass flow of 4800 lbf/sec. A mass flow of 4800 lbf/sec in turn required a fan diameter of 12.7 feet and at an axial Mach number (M_{a1}) of 0.6.

Table 12. Initial Lift Fan Parameters

Engine Parameter	
Design Point	0 feet and M=0.0
Shaft Horsepower	28300
Hub to Tip Ratio (R_h/R_t)	0.3
Inlet Stagnation Temperature ($^{\circ}\text{F}$)	518.67
Inlet Stagnation Pressure (psi)	14.696
Inlet Pressure Ratio (π_d)	0.99
Nozzle Pressure Ratio (π_n)	0.98
Fan Efficiency (e_f)	0.9

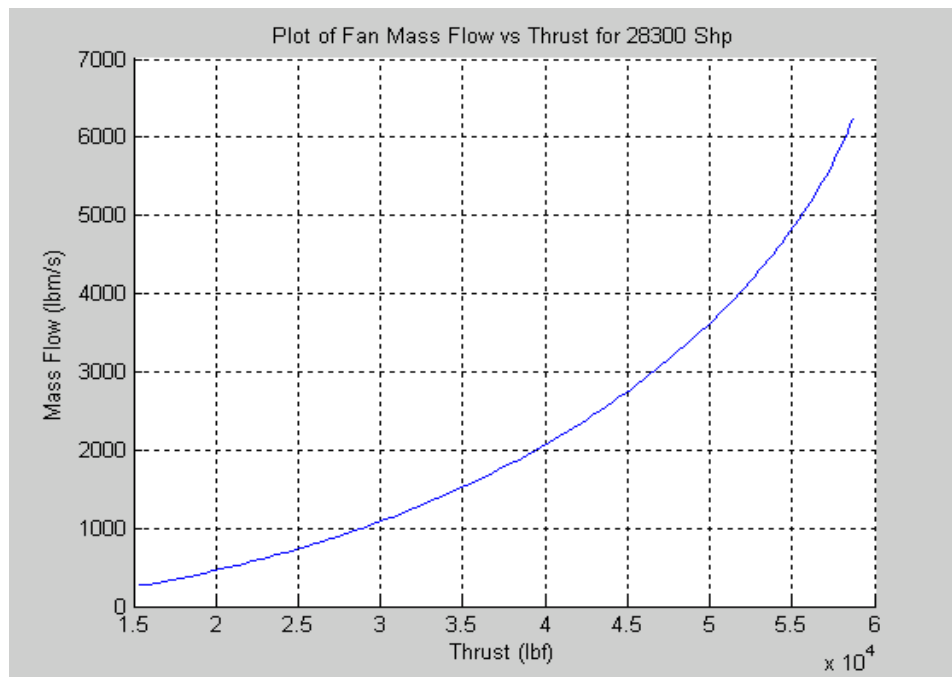


Figure 9. Mass Flow vs Thrust

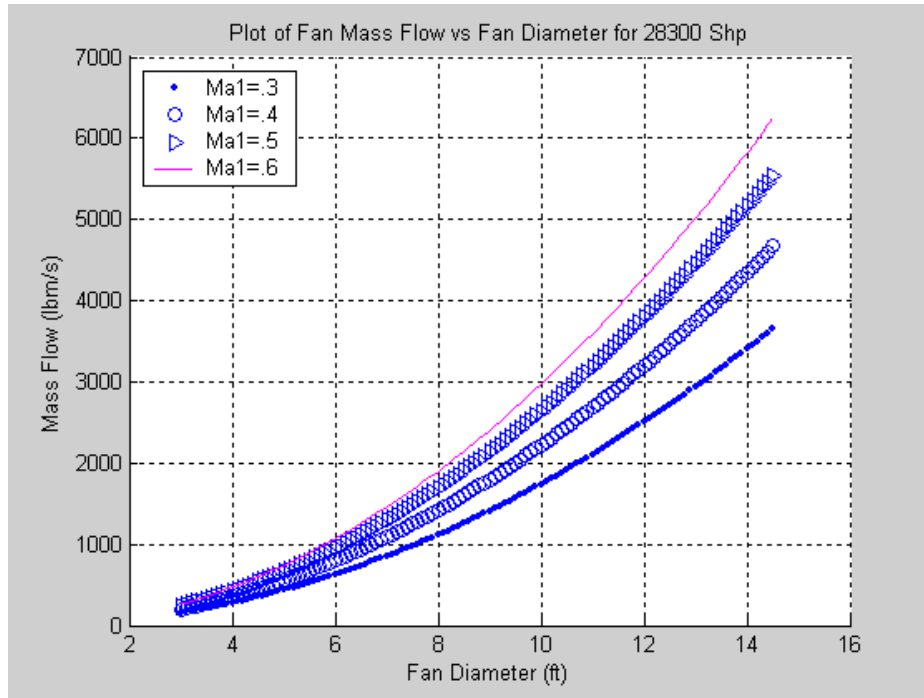


Figure 10. Mass Flow vs Lift Fan Diameter

C. LIFT FAN PRELIMINARY DESIGN

1. Design Tool

The preceding analysis gave the overall size of the lift fan. A more in depth analysis was required to determine its preliminary design. The analysis was carried out using a MATLAB 6.5 program (Aaron, Ryan, 2003). A listing of the program is given in Appendix C. The program required the following inputs: Fan blade tip speed (U_t), hub-to-tip ratio (R_h/R_t), mass flow (\dot{m}), inlet stagnation temperature (T_{t1}), inlet stagnation pressure (P_{t1}), inlet pressure drop (π_d), nozzle pressure drop (π_n), inlet relative flow angle on the meanline (β_1), rotor solidity on the meanline, stator solidity on the meanline, rotor diffusion factor on the meanline, rotor aspect ratio on the meanline and stator aspect ratio on the meanline. From these inputs the program calculated the size of the fan, the thrust provided, and velocity diagrams at hub, mean radius and tip. In using the code, the goal was to obtain the required overall thrust while not exceeding limits for the diffusion factor, at any radius, in either the rotor or stator blade row.

2. Determination of Initial Lift Fan Parameters

a. Fan Blade Tip Speed (U_t)

The fan blade tip speed was determined from the allowable centrifugal tensile stress of the fan blade. As discussed in chapter 2, paragraph B, the stress depended on the material of the blade, the flowpath throughflow area and the rotational speed. Using equation 4 and assuming the blades were made out of the titanium, a value $1.00 \times 10^{11} \text{ in}^2\text{-rpm}^2$ was calculated for AN^2 . Using equation 2 with R_h/R_t equal to 0.3 and converting rpm to ω (rad/sec), the value for AN^2 was written as

$$AN^2 = (R_t\omega)^2 = 2663811.44 \text{ ft}^2/\text{s}^2 \quad (17)$$

The maximum fan blade tip speed was $R_t\omega=1632 \text{ ft/s}$.

b. Inlet Relative Flow Angle (β_t)

The inlet relative flow angle was calculated using basic blade theory as shown in Figure 11.

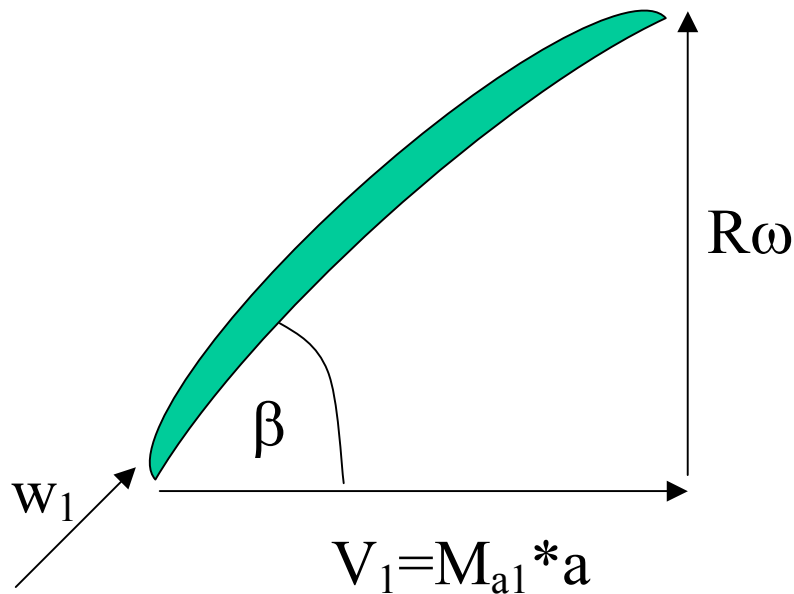


Figure 11. Basic Blade Theory

The value of β at the tip was then

$$\beta = \tan^{-1}\left(\frac{R_t\omega}{M_{a1}a}\right) = \tan^{-1}\left(\frac{R_t\omega}{M_{a1}\sqrt{\gamma RT}}\right) \quad (18)$$

With $T=518.67^\circ\text{F}$, $M_{a1}=0.6$, and $R_t\omega=1632$ ft/s, the maximum β was calculated to be 68.2 degrees.

3. Design of Lift Fan

a. Design Iteration

The design of the Lift Fan involved running the MATLAB program several times while altering the inlet mass flow (mdot), inlet relative flow angle on the meanline (β_1), rotor solidity on the meanline, stator solidity on the meanline, rotor diffusion factor on the meanline, rotor aspect ratio on the meanline and stator aspect ratio on the meanline. The purpose of each run was to maximize the thrust produced while complying with the constraints listed in Table 13.

Table 13. Lift Fan Design Constraints

Engine Parameter	
Design Point	0 feet and $M=0.0$
Maximum Shaft Horsepower	28300
Maximum Fan Blade Tip Speed (ft/s)	1632
Maximum Inlet Flow Angle on the Meanline (β_1) (deg)	68.2
Diffusion Factor at Any Point on Rotor or Stator	0.6

b. Lift Fan Gearing

Using $R_t\omega=1632$ ft/s, Table 14 showed the relationship between fan diameter and rotational speed. Previously, the LP spool of the engine was calculated to have a rotational speed of 10000 rpm. In order to limit the size of the reduction gear

between the engine and the lift fan, the lift fan was desired to operate at a minimum of 25% of the LP spool rotational speed or 2500 rpm. This rotational speed equated to a desired maximum fan diameter of 12 feet.

Table 14. Diameter vs Rotational Speed (Fan Blade Tip Speed=1632ft/s)

Lift Fan Diameter (ft)	Rotational Speed (rpm)
3	10390
6	5195
12	2597
18	1732

c. Fan Designs

Two potential designs for the lift fan are shown in Table 15. Detailed fan information is given in Table 16. The first design had a diameter of 12.1, but it did not produce the required installed thrust of 55000 lbf. The second design produced the desired amount of thrust from the lift fan, but it had a diameter of 18.4 ft and a rotational speed of 1247 rpm. The most significant parameter in the calculations was the fan blade tip speed. A high fan blade tip speed was required for smaller fan sizes and higher rotational speeds. The drawback to the high fan blade tip speed was a reduction in thrust. The first design was chosen as the final design because it met the desired rotational speed. In addition, the first design had less depth to the fan. The maximum width of both the rotor and the stator blades was 6 inches. The problem with the selection was that additional thrust was required for the aircraft to hover.

Table 15. Potential Lift Fan Designs

Engine Parameter	First Design	Second Design
Design Point	0 feet and M=0.0	0 Feet, M=0.0
Hub to Tip Ratio (R_h/R_t)	0.3	0.3
Inlet Stagnation Temperature ($^{\circ}F$)	518.67	518.67
Inlet Stagnation Pressure (psi)	14.696	14.696
Inlet Pressure Ratio (π_d)	0.99	0.99
Nozzle Pressure Ratio (π_n)	0.98	0.98
Maximum Fan Blade Tip Speed (ft/s)	1632	1200
Inlet Flow Angle on the Meanline (β_1) (deg)	62	62
Diffusion Factor on the Meanline	.205	.205
Rotor Solidity on the Meanline	0.42	.44
Stator Solidity on the Meanline	0.43	.44
Rotor Aspect Ratio on the Meanline	13	13
Stator Aspect Ratio on the Meanline	13	13
Mass Flow (lbm/s)	3910	7050
Diameter (ft)	12.1	18.4
Rotational Speed (rpm)	2576	1247
Shaft Horsepower	28005	28041
Uninstalled Thrust (lb_f)	43581	60977
Installed Thrust (lb_f)	39200	54900

Table 16. Detailed Fan Design Parameters

Engine Parameter		First Design	Second Design
Number of Rotor Blades		32	34
Rotor Blade Length (in)		50.8	77.2
Rotor Blade Width at Tip (in)		5.99	8.97
Number of Stator Blades		33	34
Stator Blade Size at Tip (in)		5.94	8.97
Rotor Diffusion Factor	At Hub	0.5967	0.5921
	At Meanline	0.205	0.205
	At Tip	0.0959	0.1680
Stator Diffusion Factor	At Hub	0.5762	0.5800
	At Meanline	0.2627	0.2645
	At Tip	0.1680	0.1690

THIS PAGE INTENTIONALLY LEFT BLANK

V. FINAL AIRCRAFT DESIGN

A. ADDITION OF THRUST

1. Requirement

The previous steps left the derivative lift fan engine design for the aircraft, short of its target. The first deficiency was the thrust required in hover. A summary of the thrust calculated in the previous chapters is provided in Table 17.

Table 17. Summary of Thrust Calculations

Installed Thrust from Poweplants (lb _f)	Installed Thrust from Lift Fans (lb _f)	Total Thrust (lb _f)	Maximum Weight of Aircraft (lbs)
61400	78400	139800	175000

The numbers showed that an additional 35200 lb_f of thrust was required to hover the aircraft at maximum weight. The second deficiency was the limited capabilities of the engines during cruise. The small margin between the thrust available and the thrust required at 20000 feet and M=0.6 (Table 7) indicated that the aircraft would have a difficult time achieving a cruise altitude of 20000 feet.

2. Solution

A proposed solution for the two deficiencies of the derivative engines was the addition of two baseline engines, having the performance given in Table 3. A summary of the additional engine's performance is shown in Table 18.

Table 18. F-35C Engine Performance

Operating Point	Uninstalled Thrust (lb _f)	Installed Thrust (lb _f)	Total Thrust (lb _f) for Two Engines
0 feet and M=0.0	33767	30400	60800
20000 feet and M=0.6	21241	19020	38040

Assuming that each engine added 6000 lbs of weight to the design, the addition of the baseline engines provided the thrust required to hover as shown in Table 19.

Table 19. Summary of Thrust Calculations

Installed Thrust from Powerplants (lb _f)	Installed Thrust from Lift Fans (lb _f)	Total Thrust (lb _f)	Maximum Weight of Aircraft (lbs)
122200	78400	200600	187000

In addition to the extra thrust for hover, the 38040 lb_f of thrust at 20000 feet and M=0.6 was significantly greater than the 19500 lbs of thrust required (Table 7). Thus, the additional engines provided an improved cruise capability at high altitudes as well as an increased hover capability.

B. DESIGN OF TRANSMISSION SHAFT

The transmission shaft was designed for the shortest length between the powerplant and the lift fan. The final shaft configuration is shown in Figure 12. Segment A was the part of the shaft that connected the powerplant and the reduction gear. It was set at 3 feet to provide room for the intake for the powerplant and it turned at 10000 rpm. Segment B was the part of the shaft that connected the reduction gear to the lift fan. It was set at 6.5 feet to provide clearance between the fan and the reduction gear. In addition, it turned at 2500 rpm. Figure 8 showed that the lengths of both shafts were satisfactory for avoiding the natural frequency of the shaft when they were turning at their designed rotational speed.

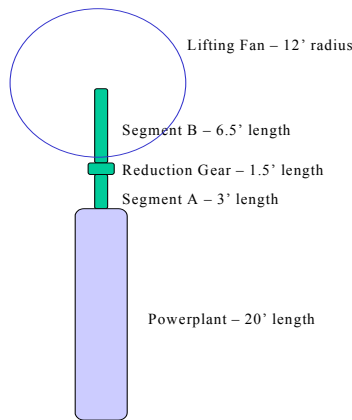


Figure 12. Lift Fan Engine Installation Dimensions

C. FINAL AIRCRAFT DESIGN

The final aircraft design was powered by two lift fan engines and two baseline engines. A diagram of the aircraft is shown in Figures 13 and 14. The important things to note were the large increase in the wing area required to incorporate the lift fan. In addition, the engines were spaced on the fuselage in order to balance the thrust with respect to the center of gravity of the aircraft.

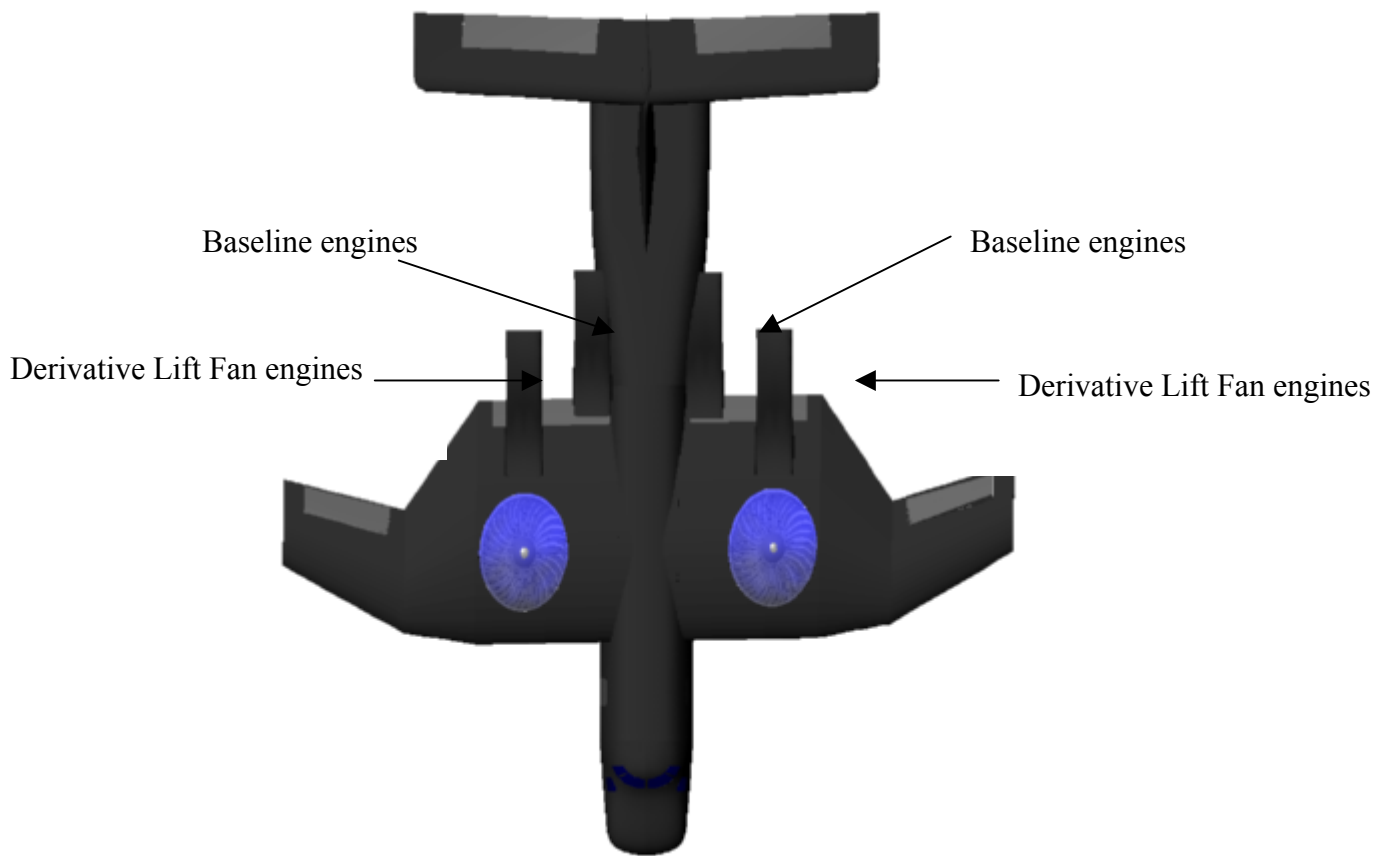


Figure 13. Top View of Heavy Lift Aircraft



Figure 14. Perspective View of Heavy Lift Aircraft

VI. CONCLUSIONS AND RECOMMENDATIONS

A. CONCLUSIONS

Current technology engines can be used in the design of lift fan engines for a heavy lift aircraft. The steps for designing derivative lift fan engines with otherwise current technology were successfully outlined in this project. The steps involved creating a derivative engine by optimizing a baseline engine for hover conditions. When the derivative engine was used to power a large lift fan, the resulting lift fan engine generated a significant amount of vertical thrust. Although the thrust from the lift fan engine was limited by aircraft constraints, it was still significantly more thrust than could be produced from a baseline engine. The addition of two derivative lift fan engines to two baseline engines provided a heavy lift aircraft with enough thrust to take-off vertically as well as cruise at speeds greater than $M=0.6$.

B. RECOMMENDATIONS

1. Perform a complete mission study in order to determine precisely the aircraft weight and fuel requirements.
2. Develop a tool to carry out the preliminary design of the LP turbine.
3. Develop tools that provide more thorough design of the transmission shaft and reduction gear.
4. Develop more tools to allow the designer to examine the aircraft structural constraints when determining the size of the lift fan.

THIS PAGE INTENTIONALLY LEFT BLANK

LIST OF REFERENCES

Aaron, Ryan, *Lift Fan Code*, developed by Prof. Ray Shreeve and converted to MATLAB by Ryan Aaron, 2003

Allen and Haisler, *Introduction to Aerospace Structural Analysis*, John Wiley & Sons, Inc., New York, NY, 1985

Den Hartog, J.P., *Mechanical Vibrations*, Dover Publications, Inc., Mineola, NY, 1985, p. 225

Erhardt, W., Draft Initial Requirements Document 2 for Aeronautical Design Project, Naval Postgraduate School, Summer Quarter 2002

Mattingly, Heiser and Pratt, *Aircraft Engine Design*, American Institute of Aeronautics and Astronautics, Inc., Reston, VA, 2002

Oates, Gordon C., *Aerothermodynamics of Gas Turbine and Rocket Propulsion*, American Institute of Aeronautics and Astronautics, Inc., Reston, VA, 1997

Wood, E. R., Faculty Advisor for *2003 Naval Postgraduate Expeditionary Warfare Aircraft Solution – Joint Heavy Lift Aircraft*, Naval Postgraduate School, Spring Quarter 2003

THIS PAGE INTENTIONALLY LEFT BLANK

APPENDIX A

Mixed Flow Turbofan Inputs

Altitude (ft)	30000
Delta T from ISA (°R)	0
Relative Humidity	0
Mach Number	1.47
<i>BASIC DATA</i>	
Intake Pressure Ratio	1
Inner Fan Pressure Ratio	5
Booster Map Type (0/1/2)	0
Outer Fan Pressure Ratio	5
Compressor Interduct Pressure Ratio	0.99
HP Compressor Pressure Ratio	6.4
Bypass Duct Pressure Ratio	0.97
Turbine Interduct Pressure Ratio	0.98
Design Bypass Ratio	0.3
Burner Exit Temperature (°R)	3760
Burner Design Efficiency	0.9995
Burner Partload Constant	1.6
Fuel Heating Value (BTU/lb)	18552.4
Handling Bleed Location	0
Overboard Bleed (lb/s)	0
Power Offtake (hp)	67.0511
HP Spool Mechanical Efficiency	1
LP Spool Mechanical Efficiency	1
Burner Pressure Ratio	0.97

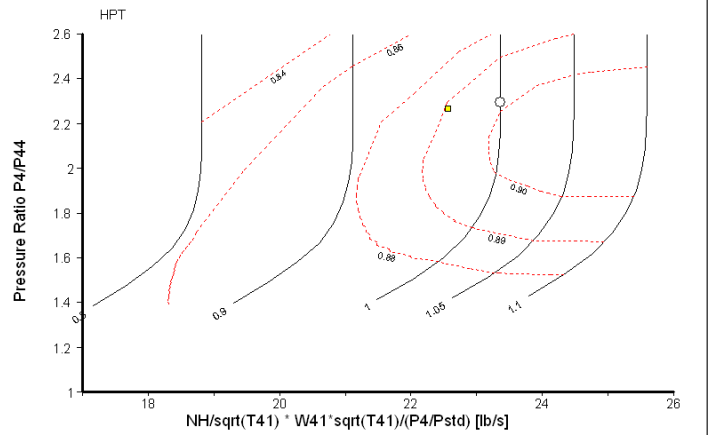
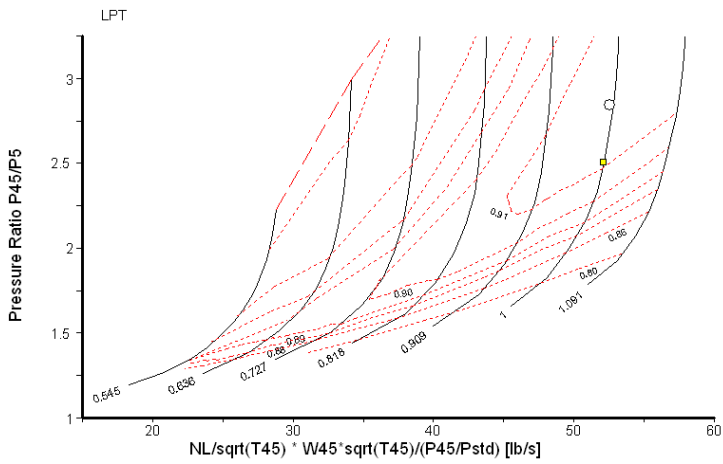
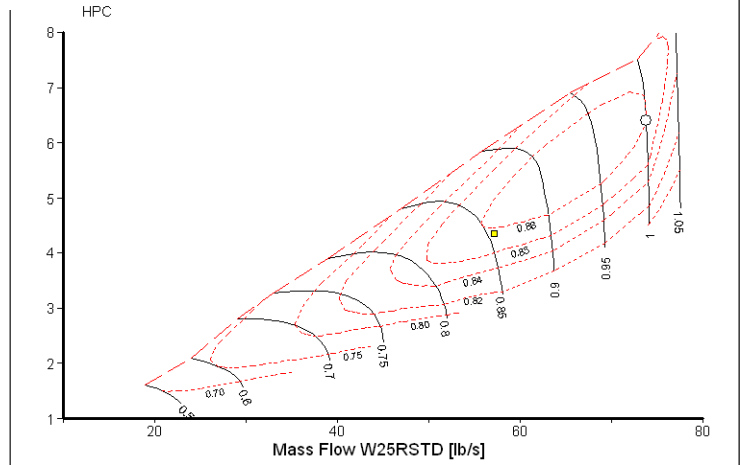
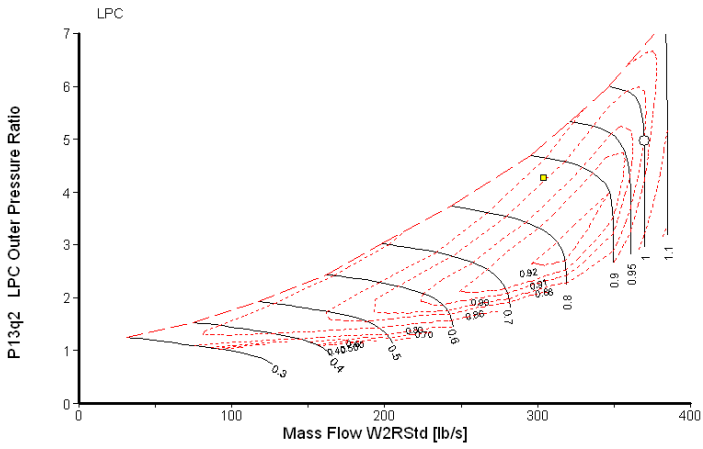
Turbine Exit Duct Pressure Ratio	0.98
Hot Stream Mixer Pressure Ratio	0.98
Cold Stream Mixer Pressure Ratio	0.99
Mixed Stream Pressure Ratio	1
Mixer Efficiency	0.5
Design Mixer Mach Number	0.2
Design Mixer Area (in ²)	0
Nozzle Thrust Coefficient	1
Design Nozzle Petal Angle (°)	25
<i>AIR SYSTEM</i>	
Relative Handling Bleed to Bypass	0
Relative Enthalpy of HP Handling Bleed	0
Relative HP Leakage to Bypass	0
Relative Overboard Bleed (W_Bld/W25)	0.005
Relative Enthalpy of Overboard Bleed	1
NGV Cooling Air (W_CL_NGV/W25)	0.05
LPT Cooling Air (W_CL/W25)	0.03
Relative Enthalpy of LPT Cooling Air	0.6
HPT Cooling Air (W_CL/W25)	0.05
Relative HP Leakage to LPT Exit	0
Relative Fan Overboard Bleed (W_Bld/W13)	0
<i>MASS FLOW INPUT</i>	
Inlet Corrected Flow (W2Rstd) (lb/s)	370
<i>LPC Efficiency</i>	
Isentropic Inner LPC Efficiency	0.89
Isentropic Outer LPC Efficiency	0.88
<i>LPC Design</i>	

Nominal LP Spool Speed	10000
<i>HPC Efficiency</i>	
Isentropic HPC Efficiency	0.86
<i>HPC Design</i>	
Nominal HP Spool Speed	18000
<i>HPT Efficiency</i>	
Isentropic HPT Efficiency	0.9
<i>LPT Efficiency</i>	
Isentropic LPT Efficiency	0.91

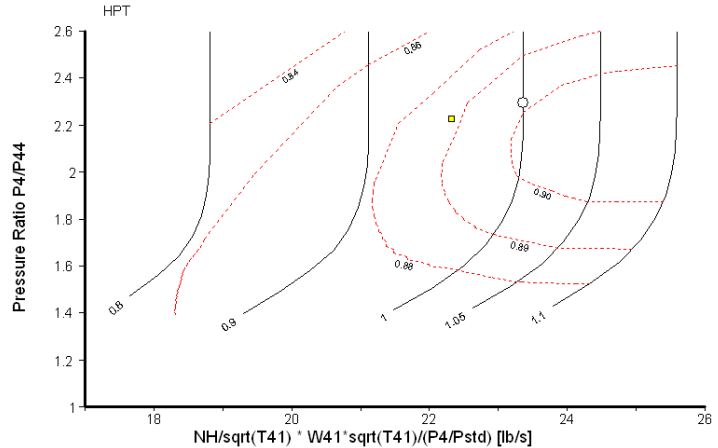
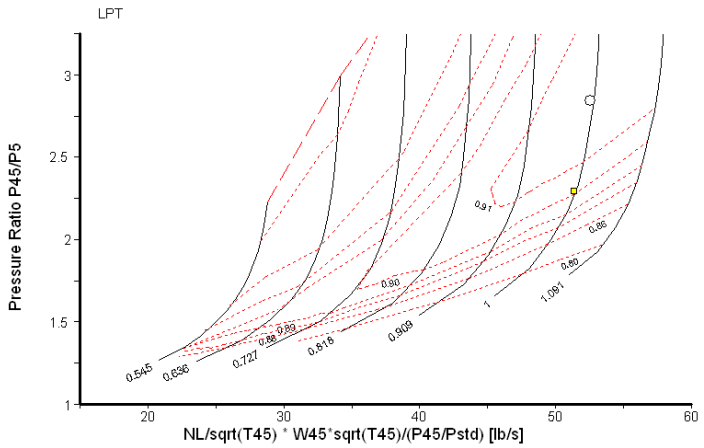
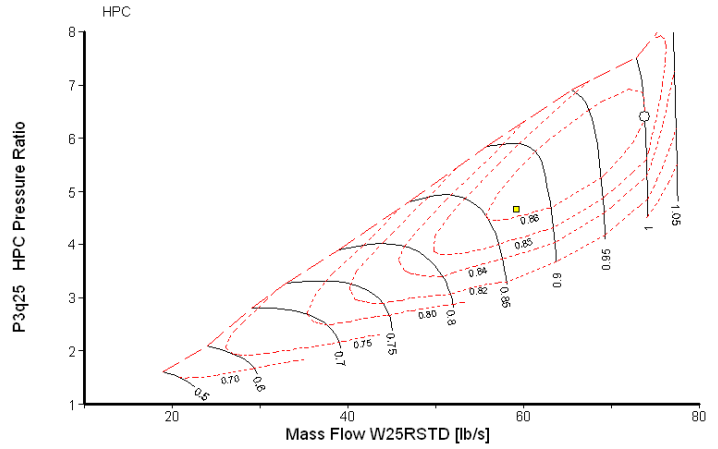
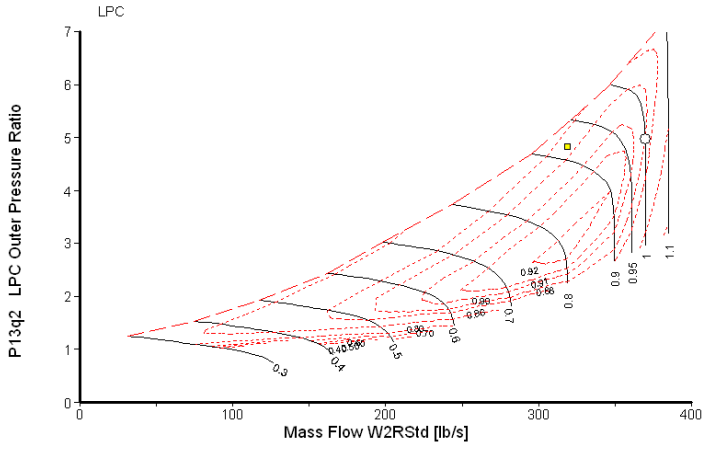
THIS PAGE INTENTIONALLY LEFT BLANK

APPENDIX B

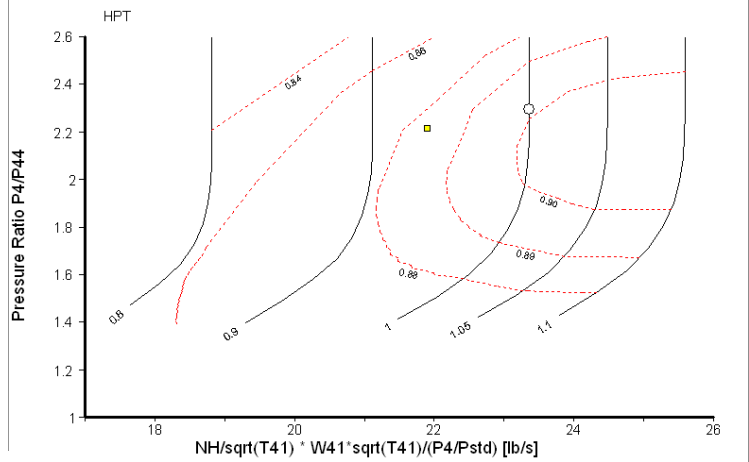
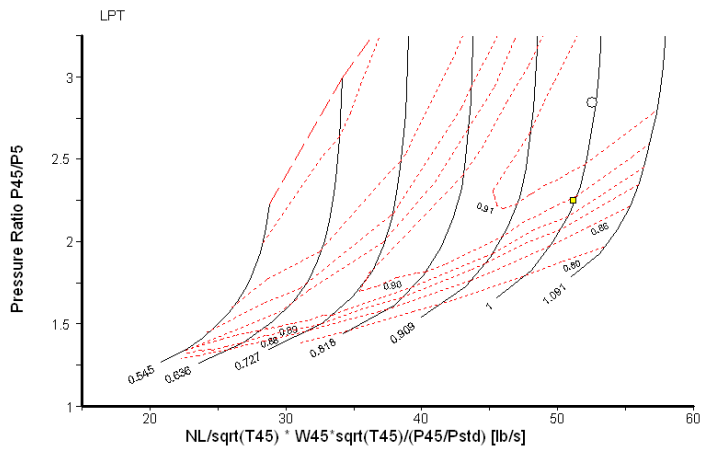
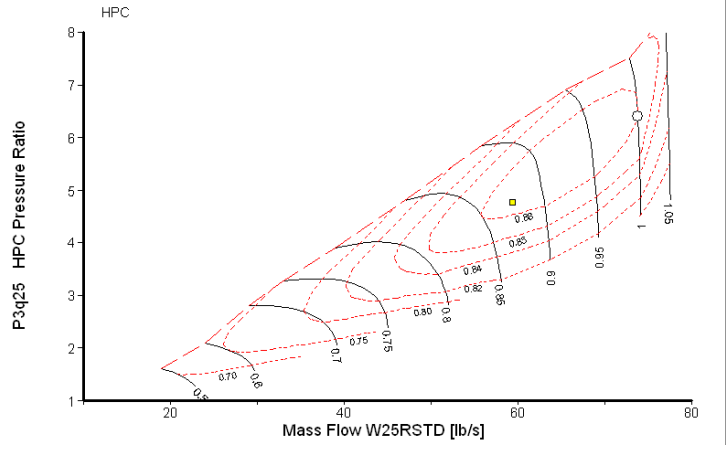
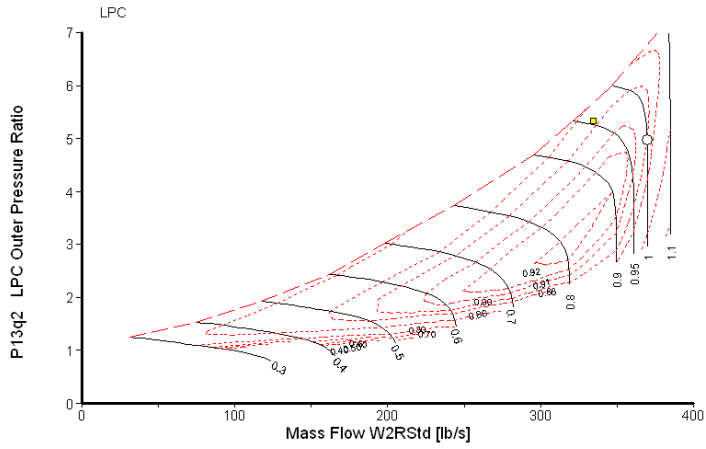
COMPONENT MAPS FOR 0 FEET AND M=0.0 (CRUISE)



COMPONENT MAPS FOR 5000 FEET AND M=0.55 (CRUISE)



COMPONENT MAPS FOR 20000 FEET AND M=0.6 (CRUISE)



THIS PAGE INTENTIONALLY LEFT BLANK

APPENDIX C

Lift Fan Code

Developed by Prof. Ray Shreeve and converted to *Matlab*® by Ryan Aaron

```
% IMPULSE STAGE COMPRESSOR DESIGN PROGRAM "CDESIGN"
% UPDATED 1-27-03 (R.P.SHREEVE) FOR LIFT FAN THRUST AND POWER
%
%-----DECLARE INTEGER VARIABLES
%-----//-----INPUT DATA STATEMENTS-----//-----
%
%-----//--NECESSARY BOUNDARY CONDITIONS--//-----
%
Utip=1000;           % WHEEL SPEED AT THE FIRST ROTOR TIP (FT/SEC)
Rhub_tip=.3;        % HUB-TO-TIP RADIUS RATIO AT THE ROTOR FACE
Kblock=.98;         % INLET BLOCKAGE FACTOR (TO ALLOW FOR HUB AND
%
%SHROUD BOUNDARY LAYERS
%
Mdot=3250;          % FLOW RATE (LBS/SEC)
Pt0=14.7;           % STAG.PRESSURE INTO FIRST ROTOR
Tt0=518.7;         % STAG.TEMP.INTO FIRST ROTOR
%
%-----//--Fan inlet and nozzle loss--//-----
%
Pid=.99;
Pin=.98;
%
%-----//--NECESSARY CONSTANTS-----//-----
%
Cp=.238;            % SPECIFIC HEAT AT CONSTANT PRESSURE
Gc=32.174;          % GRAVITATIONAL CONSTANT (LBF/LBM.FT/SEC2)
J=778;              % MECHANICAL EQUIV. OF HEAT (FT.LBS/BTU)
Gamma=1.4;          % RATIO OF SPECIFIC HEATS
%
%-----//-----SECONDARY VARIABLES-----//-----
%
Phir=1;             % RATIO OF AXIAL VEL. OUT/INTO ROTOR
Phis=1;             % RATIO OF AXIAL VEL. OUT/INTO STATOR
Lr=0;               % COEFF. OF 1/RBAR TERM IN SOLIDITY VARIATION
                    % FOR ROTOR
Ls=0;               % SAME FOR THE STATOR
Nr=0;               % COEFF. OF RBAR TERM IN SOLIDITY VARIATION FOR
                    % ROTOR
Ns=0;               % SAME FOR THE STATOR
%
%-----// PRIMARY CHOICES //-----
%
Bet1m=54.6*pi/180;  % INLET RELATIVE FLOW ANGLE ON THE MEANLINE
%
Sigrm=1.25;         % ROTOR SOLIDITY ON THE MEANLINE
Sigsm=1.25;         % STATOR SOLIDITY ON THE MEANLINE
```

```

Drm=.4636;           % ROTOR DFACTOR ON THE MEANLINE
Arr=6;              % ROTOR ASPECT RATIO ON THE MEANLINE
Ars=8;              % STATOR ASPECT RATIO ON THE MEANLINE
Clrhr=.006;        % ROTOR TIP CLEARANCE/BLADE HEIGHT
Clrhs=.006;        % STATOR TIP CLEARANCE/BLADE HEIGHT
%
%
%----INPUT COMPLETE - STAGE CALCULATION STARTS -----
%
Pt1=Pt0;
Tt1=Tt0;
%
% BEGIN THE CALCULATION OF EACH NEW STAGE HERE
%
disp('RESULTS FOR LIFT FAN');
disp('-----');
disp(' ');
disp('TIP SPEED = ');disp(Utip);disp('Ft/Sec');
disp('FLOW RATE=');disp(Mdot);disp('lbs/sec')
disp('Pt=');disp(Pt1);disp('psia');
disp('Tt=');disp(Tt1);disp('Deg.R');
disp(' ');
%
%-----START CALCULATIONS
%
%-----INLET FLOW CONDITIONS
%
Um=Utip*(1+Rhub_tip)/2;
Vt1=sqrt(2*Cp*Gc*J*Tt1);
Xulm=Um/Vt1;
Xlm=Xulm/tan(Bet1m);
M1m=FNMFfromx(Xlm,Gamma);
Mw1m=M1m/cos(Bet1m);
Mulm=M1m*tan(Bet1m);
Gammastar1=FNGGammastar(Xlm,Gamma);
A1=Mdot*Vt1/(144*Pt1*Kblock*Gc*Gammastar1);
Rm=sqrt(A1*(1+Rhub_tip)/(4*pi*(1-Rhub_tip)));
H=2*Rm*(1-Rhub_tip)/(1+Rhub_tip);
Omega=Um/Rm;
Phi1=1/tan(Bet1m);
disp('MEAN RADIUS = ');disp(Rm*12);disp(' INCHES')
disp('BLADE HEIGHT = ');disp(H*12);disp(' INCHES');
%
%-----ACROSS THE ROTOR
%
Bet2m=FNInv_dfact(Drm,Phir,Sigrm,Bet1m);
Rstm=.5*(1+(Phir*Phi1*tan(Bet2m)));
disp(' ');
disp('VELOCITY DIAGRAM: FOR BETA 1= ');disp(Bet1m);disp(' ROTOR
DFACTOR=');disp(Drm);
disp('BETA 2= ');disp(Bet2m);
Alpha1m=0;
Alpha2m=atan(2*(1-Rstm)/(Phir*Phi1));
disp('ALPHA 2= ');disp(Alpha2m);
disp(' ');

```

```

disp('REACTION= ');disp(Rstm);
X2m=Phi1*Phir*Xulm/cos(Alpha2m);
Tau=1+4*(1-Rstm)*Xulm^2;
Y2m=X2m/sqrt(Tau);
M2m=FNMfromx(Y2m, Gamma);
Mw2m=M2m*cos(Alpha2m)/cos(Bet2m);
%
%
%
%-----ACROSS THE STATOR
%
Y3m=Phis*Y2m;
M3m=FNMfromx(Y3m, Gamma);
Alpha3=0;
Dsm=FNDfact(Phis, Sigsm, Alpha2m, Alpha3);
disp('STATOR DFACTOR=');disp(Dsm);
disp(' ');
%
%-----DECIDE ON BLADE NUMBERS
%
Chordrm=H/Arr;
Zr=2*pi*Rm*Sigrm/Chordrm;
disp('NUMBER OF ROTOR BLADES IS ');disp(Zr);
Zr=input('ENTER WHOLE NUMBER REQUIRED ');
disp('CHOSEN WHOLE NUMBER IS ');disp(Zr);
Sprm=2*pi*Rm/Zr;
Chordrm=Sprm*Sigrm;
Chordsm=H/Ars;
Zs=2*pi*Rm*Sigsm/Chordsm;
disp('NUMBER OF STATOR BLADES IS ');disp(Zs);
Zs=input('ENTER WHOLE NUMBER REQUIRED ');
disp('CHOSEN WHOLE NUMBER IS ');disp(Zs);
Spsm=2*pi*Rm/Zs;
Chordsm=Spsm*Sigsm;
Spsmh=Spsm/H;
Sprmh=Sprm/H;
disp(' ');
disp('BLADING SIZES: FOR ASPECT RATIO ROTOR=');disp(Arr);disp('
STATOR=');disp(Ars);
disp(' ');
disp('ROTOR CHORD = ');disp(Chordrm*12);disp(' inches');
disp('SPACE = ');disp(Sprm*12);disp(' ');
disp('STATOR CHORD = ');disp(Chordsm*12);disp(' inches');
disp('SPACE = ');disp(Spsm*12);disp(' ');
disp(' ');
%
%-----SEC.FLOW AND T.C.LOSS FROM MEAN LINE CONDITIONS
%
Omeagarstc=FNOmegastc(Sigrm, Bet1m, Bet2m, Sprmh, Clrhr);
Omeagasstc=FNOmegastc(Sigsm, Alpha2m, Alpha3, Spsmh, Clrhs);
disp('SEC.& T.C. LOSS FOR ROTOR= ');disp(Omeagarstc);
disp('SEC.& T.C. LOSS FOR STATOR= ');disp(Omeagasstc);
disp(' ');
disp('-----');
%

```

```

%-----RADIAL DISTRIBUTION OF CONDITIONS & PERFORMANCE
%
disp(' ');
disp('HUB-TO-TIP CALCULATIONS');
disp('-----');
disp(' ');
N=2; % N=NUMBER OF STREAMLINES
disp('FOR SOLIDITY VARIATION IN THE ROTOR, Lr=');disp(Lr);disp(' and
Nr=');disp(Nr);
disp('AND IN THE STATOR, Ls=');disp(Ls);disp(' and Ns=');disp(Ns);
disp('-----');
Invn=1/N;
Rbart=2/(1+Rhub_tip);
Rbarh=Rbart*Rhub_tip;
%
%----SET UP COUNTER TO AVERAGE P.R.
%
Number=0;
Prttsum=0;
for I=0:Invn:1
Number=Number+1;
Rbar=1+(1-Rhub_tip)*(2*I-1)/(1+Rhub_tip);
disp('AT RBAR=');disp(Rbar);
X1=X1m;
Xul=Rbar*Xulm;
Xw1=sqrt((X1^2+Xul^2));
Bet1=asin(Xul/Xw1);
M1=M1m;
Mw1=M1/cos(Bet1);
Alpha2=atan(tan(Alpha2m)/Rbar);
Bet2=atan((Rbar/(Phi1*Phir))-tan(Alpha2m)/Rbar);
Y2=Y2m*cos(Alpha2m)/cos(Alpha2);
M2=FNMfromx(Y2, Gamma);
Mz2=M2*cos(Alpha2);
Mw2=Mz2/cos(Bet2);
Yw2=FNXfromm(Mw2, Gamma);
Y3=Y2*cos(Alpha2)*Phis;
M3=FNMfromx(Y3, Gamma);
Sigr=Sigrm*(Lr+Rbar+Nr*Rbar^2)/Rbar; % VARIATION IN SOLIDITY
Sigs=Sigsm*(Ls+Rbar+Ns*Rbar^2)/Rbar; % VARIATION IN SOLIDITY
Dr=FNDfact(Phir, Sigr, Bet1, Bet2);
Ds=FNDfact(Phis, Sigs, Alpha2, Alpha3);
disp(' ');
disp('VELOCITY DIAGRAM:');
disp('BETA 1 = ');disp(Bet1);
disp('BETA 2 = ');disp(Bet2);
disp('ALPHA2 = ');disp(Alpha2);
disp(' ');
disp('ROTOR DFACTOR = ');disp(Dr);
disp('STATOR DFACTOR = ');disp(Ds);
%
% CALCULATE BLADE SIZES
%
Spr=Sprm*Rbar;
Sps=Spsm*Rbar;

```

```

Chordr=Spr*Sigr;
Chords=Sps*Sigs;
disp(' ');
disp('BLADE SIZES:');
disp('ROTOR CHORD = ');disp(Chordr*12);disp('ins. ');
disp('SPACING = ');disp(Spr*12);disp('ins. ');
disp('SOLIDITY = ');disp(Sigr);
disp('STATOR CHORD = ');disp(Chords*12);disp('ins. ');
disp('SPACING = ');disp(Sps*12);disp('ins. ');
disp('SOLIDITY = ');disp(Sigs);
disp(' ');
%
%
%---PERFORMANCE
%
Gog1=Gamma/(Gamma-1);
T1tt1=1-X1^2;
Plpt1=(1-X1^2)^Gog1;
Tr1tt1=T1tt1+Xw1^2;
Pr1pt1=Tr1tt1^Gog1;
%
%---TEST FOR SHOCK AND SHOCK LOSS
%
if Mw1>1
Spratio=FNShockprratio(Mw1,Gamma);
Pr1pt1=Pr1pt1*Spratio;
Spratio=FNShockprratio(Mw1,Gamma);
Plpt1=Plpt1*Spratio;
disp('A SHOCK WAS FOUND AT MW1=');disp(Mw1);
disp('PR(T-T) = ');disp(Spratio);disp(' PR(S-S) = ');disp(Spratio);
end
% AFTER SHOCK CONDITIONS FROM HERE
Omegap=FNOmegap(Dr,Sigr,Bet1,Bet2);
Omegart=Omegap+Omegartc;
Pr2pt1=Pr1pt1-Omegart*(Pr1pt1-Plpt1);
Tr2tt1=Tr1tt1;
T2tt1=Tr2tt1-Yw2^2;
P2pt1=((T2tt1/Tr2tt1)^Gog1)*Pr2pt1;
Pt2pt1=P2pt1/((T2tt1/Tau)^Gog1);
%
%-----ACROSS THE STATOR
%
Omeasp=FNOmegap(Ds,Sigs,Alpha2,Alpha3);
Omeast=Omeasp+Omeastc;
Pt3pt1=Pt2pt1-Omeast*(Pt2pt1-P2pt1);
Tt3tt1=Tau;
disp('PT3/PT1 = ');disp(Pt3pt1);
disp(' ');
disp('-----');
Prttsum=Pt3pt1+Prttsum;
end
Prttavg=Prttsum/Number;
disp('AVERAGE PRESSURE RATIO(T-T) = ');disp(Prttavg);
%
%-----CALCULATE CONDITIONS FOR NEXT STAGE

```

```

%
Kblock3=.98;           %BLOCKAGE FACTOR
Vt3=Vt1*sqrt(Tau);
X3m=X1m/sqrt(Tau);
Gammastar3=FNGammastar(X3m, Gamma);
A3oa1=(Gammastar1/Gammastar3)*(Kblock/Kblock3)*(sqrt(Tau))/Prttavg;
A3=A3oa1*A1;
%
%
%
%-----INPUT FRACTIONAL MEAN RADIUS CHANGE
%
Rfraction=input('ENTER FRACTIONAL MEAN RADIUS CHANGE FOR NEXT STAGE');
Rm3=Rm*Rfraction;
H3=A3/(2*pi*Rm3);
Ho2rm=H3/(2*Rm3);
Rhub_tip3=(1-Ho2rm)/(1+Ho2rm);
Um3=Um*Rfraction;
Utip3=Um3*(1+Ho2rm);
Beta3m=atan(Um3/(X3m*Vt3));
Pt3=Pt1*Prttavg;
Tt3=Tt1*Tau;
Pi0=Pt3/Pt0;
Tau0=Tt3/Tt0;
Diatip=Rm+H/2;
Diatip3=Rm3+H3/2;
%
% Calculate fan performance if correctly expanded nozzle was added here
%
Xe=sqrt(1-(1/(Pid*Pin*Pi0))^(1/Gog1));
Thrust=Mdot*Xe*Vt3/Gc;
Hpower=Mdot*Cp*Tt0*(Tau0-1)*778/550;
disp(' ');
disp('OVERALL PRESSURE RATIO [T-T] = ');disp(Pi0);
disp('OVERALL TEMPERATURE RATIO [T-T]= ');disp(Tau0);
disp(' ');
disp('Fan Diameter = ');disp(Diatip*2);disp(' inches');
disp('Fan Static Thrust [=m*Ve/gc] = ');disp(Thrust);disp(' lbsf');
disp('Fan drive horse power = ');disp(Hpower);disp(' HP');
disp(' ');
disp('FOR NEXT STAGE:');
disp('TIP DIAMETER = ');disp(Diatip3*12);disp(' inches');
disp('TIP SPEED = ');disp(Utip3);disp(' FT/SEC');
disp('MEAN RADIUS = ');disp(Rm3*12);disp(' INCHES');
disp('HUB-TIP RATIO = ');disp(Rhub_tip3);
disp('STAG.PRESSURE = ');disp(Pt3);disp(' PSIA');
disp('STAG.TEMP. = ');disp(Tt3);disp(' DEG.R');
disp('BETA (MEAN-LINE)= ');disp(Beta3m);disp(' DEG. ');
disp(' ');
disp(' ');
Xxx=input('ENTER 1 FOR ANOTHER STAGE');
Utip=Utip3;
Rhub_tip=Rhub_tip3;
Pt1=Pt3;
Tt1=Tt3;

```

Bet1m=Beta3m;

Function Calls:

```
function X=FNXfromm(M, Gamma)
X=(Gamma-1)*M*M/2;
X=X/(1+X);
X=sqrt(X);
%
function Shockpratio=FNShockpratio(Mw1, Gamma);
Msq=Mw1^2;
Ga1=(Gamma+1)/2;
Ga2=(Gamma-1)/2;
Ga3=2*Gamma/(Gamma+1);
Ga4=Gamma/(Gamma-1);
Ga5=1/(1-Gamma);
Shockpratio=((Ga1*Msq/(1+Ga2*Msq))^Ga4)*((Ga3*Msq-Ga2/Ga1)^Ga5);
%
function Shockpratio=FNShockpratio(Mw1, Gamma);
Msq=Mw1^2;
Ga3=2*Gamma/(Gamma+1);
Ga6=(Gamma-1)/(Gamma+1);
Shockpratio=Ga3*Msq-Ga6;
%
function Omegastc=FNOmegastc(Sig, B1, B2, Spch, Clrh);
Binf=atan(.5*tan(B1)+.5*tan(B2));
Cl=2*(tan(B1)-tan(B2))*cos(Binf)/Sig;
Cdi=.04*Cl*Cl*Sig*Spch+.25*Cl*Cl*Sig*Clrh/cos(B2);
Omegastc=Cdi*Sig*(cos(B1))^2/(cos(Binf))^3;
%
function Omegap=FNOmegap(D, Sig, B1, B2);
Omegap=2*Sig*(cos(B1))^2*(.005+.16*D^4)/((cos(B2))^3);
%
function M=FNMfromx(X, Gamma);
M=sqrt((2/(Gamma-1))*X^2/(1-X^2));
%
function Bet2=FNInv_dfact(D, Phi, Sig, Bet1);
A=(1-D+sin(Bet1)/(2*Sig))/Phi;
B=A^2+((cos(Bet1))^2)/(4*Sig^2);
C=(1+sqrt(1-(1-1/(4*Sig^2))*B/A^2))*A*cos(Bet1)/B;
Bet2=acos(C);
%
function Gammastar=FNGammaStar(X, Gamma);
Gammastar=(2*Gamma*X/(Gamma-1))*(1-X^2)^(1/(Gamma-1));
%
function D=FNDfact(Phi, Sig, Bet1, Bet2);
D=1-Phi*cos(Bet1)/cos(Bet2)+(tan(Bet1)-Phi*tan(Bet2))*cos(Bet1)/(2*Sig);
```

THIS PAGE INTENTIONALLY LEFT BLANK

INITIAL DISTRIBUTION LIST

1. Defense Technical Information Center
Ft. Belvoir, VA
2. Dudley Knox Library
Naval Postgraduate School
Monterey, CA
3. Dr. Raymond Shreeve
Naval Postgraduate School
Monterey, CA
4. Dr. E. R. Wood
Naval Postgraduate School
Monterey, CA
5. Dr. Phil DePoy
Naval Postgraduate School
Monterey, CA
6. Prof Charles Calvano
Naval Postgraduate School
Monterey, CA
7. Dr. Paul Bevilaqua
Lockheed Martin Skunk Works
Palmdale, CA
8. Charles C Crawford
Aerospace Transportation & Advanced Systems Laboratory
Atlanta, GA
9. Mike Hirschberg
CENTRA Technology, Inc.
Arlington, VA
10. Phil Hunt
Booz Allen Hamilton
Arlington, VA
11. Sam Wilson
DARPA
Arlington, VA